

UCSF

UC San Francisco Electronic Theses and Dissertations

Title

Arginase-I expression by innate lymphoid cells during fetal development, adult homeostasis, and inflammation

Permalink

<https://escholarship.org/uc/item/1057z1tf>

Author

Bando, Jennifer Kaoru

Publication Date

2014

Peer reviewed|Thesis/dissertation

Arginase-I expression by innate lymphoid cells during fetal
development, adult homeostasis, and inflammation

by

Jennifer Kaoru Bando

DISSERTATION

Submitted in partial satisfaction of the requirements for the degree of

DOCTOR OF PHILOSOPHY

in

Biomedical Sciences

in the

GRADUATE DIVISION

of the

UNIVERSITY OF CALIFORNIA, SAN FRANCISCO

Copyright 2014

by

Jennifer K. Bando

To my parents,
Kinichi and Haruyo

Acknowledgements

There are many people at UCSF I would like to thank for their support during my graduate studies. First, I would like to thank my mentor, Dr. Richard Locksley, for many years of guidance, patience, and encouragement. Rich's integrity, creativity, and passion for all kinds of science (from tardigrade biology to astronomy) is truly inspiring. Thank you Rich for emphasizing the importance of being independent and critical, and for believing in me. This dissertation would not have been possible without my incredible thesis committee members, Drs. Tony DeFranco, Jason Cyster, and Averil Ma, who made sure that my projects were progressing forward and gave me invaluable scientific and career advice. Dr. Lewis Lanier was extremely generous with his time during my qualifying exams and during the drafting of the fetal arginase-I paper. The Rosen, MacKenzie, and Cyster labs provided many tools, reagents, and techniques. Drs. Steve Rosen and Michael Patnode gave me access to their fluorescent dissecting microscope, Drs. Tippi MacKenzie and Marta Wegorzewska performed *in utero* injections and discussed experiments with me, and Drs. Jason Cyster, Betsy Gray and Andrea Reboldi gave me reagents and protocols.

Rich's lab has been a major source of scientific and moral support over the years. Dr. Brandon Sullivan mentored me during my first years in the lab, and taught me how to do experiments and approach technical challenges. Drs. Lee Reinhardt and Suk-Jo Kang provided guidance on how to establish new projects. Our lab would not be able to function without Dr. Hong-Erh Liang, who constantly works to improve how we do research. Previous and current students Dr. Davina Wu, Dr. April Price, Dr. Alex Mohapatra and Jinwoo Lee were incredibly encouraging and gave me advice on how to

navigate through graduate school. To my benchmates, April and Dr. Jakob von Moltke, thank you for making our bay a fun place to work and for supporting me through my successes and failures. I would not have been able to get by without Drs. Laurence Cheng, Adam Savage, Ari Molofsky, Jesse Nussbaum, and Steve Van Dyken, who were always happy to discuss experiments or take a break from work. Dr. Zhi-en Wang performed cell sorts for the lung arginase-I experiments and provided entertaining stories about the history of the lab. Ming Ji and Marites Consengco maintained my animals and were wonderful company to be around.

Working near the Matloubian and Weiss labs has been scientifically and socially enriching. I'd especially like to thank Dr. Joyce Hu, Dr. Jon Clingan, Dr. Ying-Xim Tang, Kasia Skrzypczynska, Marianne Mollenauer, and Dr. Lyn Hsu for reagents and protocols, and for many laughs over the years.

I am indebted to Lisa Magargal and Monique Piazza, the Biomedical Sciences Program administrators, and Christina Liu, a previous lab administrative assistant, for making sure that everything ran smoothly during my time as a graduate student.

Outside of the lab, I'd like to thank Drs. Joyce Hu and Jan Lui for their incredible friendship since the beginning of graduate school. Thank you Laraine Ignacio, Joanna Chan, Karena Bui, Darryl Sarmiento, Lili Harbottle, and Nai Saepanh, and Christina Kaoh for being strong women in my life and my emotional support system. Alex Habito, Lisa Tang, Lynn Duong, Brian Tran, Arthur Tran, and David Law are friends I grew up with who continue to support me in my endeavors. To my parents, Kinichi and Haruyo, and my sisters, Jun and Maki, thank you for fostering my curiosity in science and for encouraging me to find my own path.

Michael, thank you for being by my side through it all. Thank you for cheering me on, for giving me strength during difficult times, and for your unconditional love and support. This would not have been possible without you.

Contributions to Presented Work

Chapter 2 was published as “Type 2 innate lymphoid cells constitutively express arginase-I in the naïve and inflamed lung” in the Journal of Leukocyte Biology, with co-authors Drs. Jesse C. Nussbaum, Hong-Erh Liang, and Richard M. Locksley. Drs. Jesse Nussbaum and Hong-Erh Liang contributed the Red5 (IL-5) reporter mouse, and Dr. Hong-Erh Liang contributed the Arg1^{YFP} reporter mouse. I designed the study and performed the experiments. I wrote the manuscript, which was revised by Dr. Richard Locksley.

Chapter 3 was submitted for publication as “Identification and distribution of ILC precursors in the fetal mouse intestine,” with co-authors Drs. Hong-Erh Liang and Richard M. Locksley. Dr. Hong-Erh Liang contributed the Arg1^{YFP} reporter mouse. Dr. Richard Locksley and I designed the experiments, which I performed. I wrote the manuscript, which was revised by Dr. Richard Locksley.

Arginase-I expression by innate lymphoid cells during fetal development, adult homeostasis, and inflammation

Jennifer Kaoru Bando

Abstract

Innate lymphoid cells (ILCs) are a family of immune cells involved in development, homeostasis, and the host response to pathogens. In order to identify subsets of these cells *in situ* and genetically target them, additional markers for ILCs need to be established. Here, I demonstrate that arginase-I (Arg1), a urea cycle enzyme induced in alternatively activated macrophages, is expressed by multiple ILC lineages in the fetal and adult mouse. In the adult lung, group 2 ILCs (ILC2s) express Arg1 at rest and during type 2 inflammation induced by the parasitic helminth *Nippostrongylus brasiliensis*. While macrophages induce Arg1 through STAT6 activation, ILC2s express Arg1 in a STAT6-independent manner. Total numbers of Arg1⁺ cells in the lung are regulated by IL-33, which elevates ILC2 numbers and indirectly induces Arg1 expression in macrophages through activation of STAT6. Arg1 expression in ILC2s may provide a way to target these cells without altering T cell responses.

In fetal development, specialized members of group 3 ILCs (ILC3s), lymphoid tissue inducer (LTi) cells, are required for lymph node and Peyer's patch organogenesis, but how LTi cells develop at these sites remains unclear. Here, we identify an Arg1⁺, Id2⁺ ILC population in the fetal intestine that can differentiate into IL-7R α ⁺NK1.1⁺T-bet⁺ group 1 ILCs (ILC1s), GATA3^{hi} ILC2s, and ROR γ t⁺ group ILC3s *in vitro*. Based on transcription factor expression, ILC precursors in the fetal intestine represent an intermediate developmental stage between T-bet⁻ROR γ t⁻ ILC precursors

and differentiated ILC lineages. These ILC precursors outnumber other innate lymphoid populations in the intestine at embryonic day (E) 13.5. At E16.5, after the initiation of Peyer's patch organogenesis, intestinal ILC precursors accumulate at the Peyer's patch anlage in a manner that is dependent on lymphotoxin- α (LT α). Thus, during development, ILC precursors accumulate in the intestine, where they aggregate at sites of lymphoid tissue organogenesis and differentiate into mature ILC lineages.

Table of Contents

Chapter 1: Introduction.....	1
Chapter 2: Type 2 innate lymphoid cells constitutively express arginase-I in the naïve and inflamed lung.....	16
Chapter 3: Identification and distribution of innate lymphoid cell precursors in the fetal intestine.....	40
Chapter 4: Discussion.....	70
References.....	80

List of Figures

Chapter 2:

Fig 1. <i>Arginase-I</i> is expressed by type 2 innate lymphoid cells and alternatively activated macrophages in the lung during <i>N. brasiliensis</i> infection.....	21-22
Supplementary Fig 1. Assessment of alternatively activated macrophage marker expression by type 2 innate lymphoid cells.....	23
Fig 2. Type 2 innate lymphoid cells constitutively express <i>arginase-I</i>	25-26
Fig 3. <i>Arginase-I</i> deficiency does not affect type 2 innate lymphoid cell numbers or cytokine production.....	28-29
Fig 4. <i>IL-33</i> can regulate <i>arginase-I</i> ⁺ cell numbers in lung tissue.....	32

Chapter 3:

Fig. 1. <i>Arginase-I</i> is expressed by LTI-like cells in cryptopatches.....	45
Fig. 2. <i>Arginase-I</i> expression marks innate lymphoid populations in the fetal mouse gut.....	47
Supplementary Fig. 1. Characterization of <i>Arg1</i> ^{YFP+} <i>NK1.1</i> ⁺ cells.....	49
Fig. 3. Fetal <i>Arg1</i> ^{YFP+} <i>RNT</i> ⁻ cells aggregate at the Peyer's patch anlage in a lymphotoxin-dependent manner.....	51-52
Supplementary Fig. 2. <i>Arginase-I</i> is not required for Peyer's patch development.....	54
Fig. 4. Characterization of <i>Arg1</i> ^{YFP+} <i>RNT</i> ⁻ cells.....	56
Fig. 5. <i>Arg1</i> ^{YFP+} <i>RNT</i> ⁻ cells are fetal ILC precursors.....	58-59
Fig. 6. <i>Arg1</i> ^{YFP} expression by ILC precursors in fetal liver and adult bone marrow.....	61

Discussion

Fig. 1. Model of ILC precursor localization during Peyer's patch development.....	74
-----------------------------------------------------------------------------------	----

Chapter One:

Introduction

Innate lymphoid cells

The immune system is essential for host protection against pathogens, regulation of commensal populations, and maintenance of homeostatic processes. In vertebrates, the immune system consists of both innate and adaptive cell populations (Cooper & Alder, 2006). Adaptive immune cells such as T and B cells are antigen-specific, exhibit immunologic memory, and express receptors encoded by somatically recombined genes, while innate cells in general lack these characteristics and instead respond to activating cytokines, conserved molecules expressed by pathogens, and molecules expressed by infected or stressed cells (Medzhitov & Janeway, 2000). In gnathostomes (jawed vertebrates), somatic gene rearrangement in adaptive immune cells is dependent on recombination activating gene (*Rag1/Rag2*) products. (Cooper & Alder, 2006; Schatz & Ji, 2011). This process of receptor gene rearrangement not only functionally separates innate and adaptive cells, but also distinguishes these two groups of immune cells based on developmental requirements; *Rag1*- and *Rag2*-deficient mice lack adaptive lymphocytes, while the innate compartment remains intact with the exception of innate-like T cells (Mombaerts et al, 1992; Shinkai et al, 1992). The innate lymphoid cell (ILC) is a class of immune cell described in the human and mouse that shares characteristics with both innate and adaptive cell types. ILCs are functionally innate because they do not express receptors encoded by somatically rearranged genes nor do they require RAG genes for their development (Fuchs et al, 2013; Moro et al, 2010; Satoh-Takayama et al, 2008; Takatori et al, 2009). However, ILCs are similar to adaptive lymphoid cells in that they share a common progenitor with T cells and B

cells (Klose et al, 2014), require the common gamma chain for their development and survival (Spits & Di Santo, 2011), and appear lymphocytic by morphology.

ILCs have been a focus of intense interest in recent years due to the discovery that they produce cytokines that mirror those expressed by helper T cells. Thus, different subtypes of ILCs have been defined based on cytokine and transcription factor expression in a manner similar to how helper T cells subsets are categorized (Spits et al, 2013) (Fig. 1). Group 1 ILCs (ILC1s) express the transcription factor T-bet, produce the cytokine IFN γ , and have been implicated in the immune response to bacteria and viruses. Group 2 ILCs (ILC2s) express ROR α and high levels of GATA3; produce IL-5, IL-9, and IL-13; and contribute to allergy, the response to parasitic helminths, and the maintenance of homeostasis. Group 3 ILCs (ILC3s) express ROR γ t, produce IL-17 and IL-22, and are important in mucosal immunity and integrity as well as lymphoid tissue organogenesis. Because specific antigen is not required for the direct activation of ILCs, these cells have been proposed to be an early source of cytokines in tissue during immune activation.

Group 1 innate lymphoid cells

ILCs that express T-bet and produce IFN γ consist of several NK-receptor-expressing populations, including classical NK cells (cNK), NK1.1⁺NKp46⁺ intraepithelial ILCs, NKp46⁺T-bet⁺ ILCs that are derived from ROR γ t⁺ cells (“ex-ROR γ t” ILCs), and NK1.1⁺NKp46⁺IL-7R α ⁺ ILCs that never express ROR γ t. These populations differ in their expression of the transcription factors eomesodermin (Eomes) and ROR γ t, and requirements for IL-15. cNK cells require Eomes and IL-15 for development, and produce high levels of granzyme B after activation (Gordon et al, 2012; Kennedy et al,

2000). In contrast to other ILCs, which are dependent on *Id2* for their lineage specification, cNK precursors still develop in the bone marrow of *Id2*^{-/-} mice, although mature peripheral cNK cells are absent in knock out animals (Boos et al, 2007). Out of the three non-cNK T-bet⁺ ILC populations, intraepithelial ILCs, which express CD160 and produce IFN γ in response to IL-12 and IL-15, are perhaps the most closely related to cNK cells based on their shared expression of *Eomes* in human and dependence on *Nfil3* in mouse (Fuchs et al, 2013). However, these cells differ from cNK cells because they still develop in the absence of IL-15R α . *Id2* requirements have not yet been tested for this population. Ex-ROR γ t ILCs and IL-7R α ⁺ ILC1s that do not fate map for ROR γ t expression are both *Eomes*-negative and are dependent on IL-15 (Klose et al, 2014; Klose et al, 2012; Rankin et al, 2013). Since ex-ROR γ t ILCs transition out of the ILC3 pool, and thus do not exist in ROR γ t-deficient animals, it has been proposed that these cells should be labeled ILC3s. IL-7R α ⁺NK1.1⁺ ILC1s that do not fate map for ROR γ t produce IFN γ and TNF in response to IL-12, and are a terminally differentiated population since they do not differentiate into *Eomes*⁺ cNK cells or ROR γ t⁺ ILC3s after adoptive transfer (Klose et al, 2014).

The definition of what constitutes a group 1 ILC member remains controversial. ILC1s were initially defined as all innate lymphoid populations that express T-bet and produce IFN γ , and thus cNK cells and other T-bet⁺ ILC populations were included in this group (Spits et al, 2013). However, more recently, Andreas Diefenbach proposed that ILC groups should only include developmentally related IL-7R α ⁺ cells that are derived from a shared precursor (Klose et al, 2014). Taking into account the reasoning that ex-ROR γ t ILCs are ILC3s, this definition of ILC1s would restrict this group to consist of only

IL-7R α ⁺T-bet⁺Eomes⁻ non-ROR γ t-fate mapped ILCs. The designation of ILC1s based on developmental definitions is logical, especially since the classification of ILC groups is modeled after mature T helper cell subsets, which differentiate from naïve T cells. However, until there is a clear consensus that these definitions should be altered, all innate lymphoid populations that are T-bet⁺, but independent of cell-intrinsic ROR γ t, will continue to be categorized as ILC1s.

Group 2 innate lymphoid cells

Type 2 immune responses to parasitic helminths or allergic particles are characterized by enhanced mucus output, smooth muscle contraction, eosinophilia, and IgE production. ILC2s are Lineage (Lin)⁻IL-7R α ⁺ckit⁺KLRG1⁺T1/ST2⁺CD25⁺ tissue resident cells that can contribute to many of these physiological responses by producing IL-5, which is required for eosinophil development and survival, and IL-13, which induces alternative activation of macrophages, regulates eosinophil entry into tissue, and activates mucus cell hyperplasia and smooth muscle contraction (Erle & Sheppard, 2014; Molofsky et al, 2013). These cells were first reported under various names including nuocytes, innate helper type 2 cells, and natural helper cells (Moro et al, 2010; Neill et al, 2010; Price et al, 2010), but were proposed to be a single population based on their dependence on the transcription factor ROR α and GATA3; requirements for the epithelial cytokines IL-33 and IL-25; and production of IL-5, IL-9, and IL-13 (Spits et al, 2013). During infection with the parasitic helminth *Nippostrongylus brasiliensis*, ILC2s are the predominant IL-13 producers in the early response in the lung (Neill et al, 2010). Adoptively transferred ILC2s are sufficient to rescue worm clearance in IL-25-receptor

deficient *IL-17br/-* animals by providing IL-13 (Neill et al, 2010), and drive eosinophilia and worm expulsion in *Rag2//I2rg* double knockout animals (Price et al, 2010).

Although it is clear that ILC2s are a source of IL-5 and IL-13 during worm infection, the significance of this contribution under physiological conditions in systems where T cells are activated is still unclear, since there are currently no reagents available that specifically target ILC2s without altering T cell function. ROR α -deficient *staggerer* mice lack ILC2s, and cells from these mutant mice have been used in BM transfer systems as ILC2-deficient models (Halim et al, 2012; Wong et al, 2012), but it remains unclear whether ROR α ^{-/-} Th2 cells respond normally in these mice in vivo. Indeed, skewed cytokine production in CD8 T cells, mast cells, and macrophages in *staggerer* mice indicate that these mice have widespread immune dysregulation (Dzhagalov et al, 2004). Additionally, the IL-5 reporter Red5 and the IL-13 reporter Yetcre13 crossed with Rosa26-DT α mice produce animals that are depleted of IL-5- or IL-13-producing ILC2s, respectively (Molofsky et al, 2013; Price et al, 2010). However, these animals also have reduced Th2 cells that express these cytokines. Thus, although these animal models are extremely useful tools for studying these rare cells, new markers for ILC2s are required to better interrogate the functional consequences of ILC2 depletion in the context of intact T cell function. In Chapters 2 and 3, I show that the enzyme arginase-I (Arg1) is constitutively expressed by ILC2 cells throughout development, and not by Th2 cells. Genes that are differentially expressed in ILC2s and Th2 cells, such as Arg1, may provide ways to target ILC2 functions in vivo.

Group 3 innate lymphoid cells

ILC3s are ROR γ ⁺ mucosal tissue- and lymphoid organ-resident cells that include lymphoid tissue inducer (LTi) cells, NKp46⁺ cells that produce IL-22 (NK-22), and ex-ROR γ ⁺ ILCs that express T-bet and IFN γ . LTi cells in the fetus, and their adult counterpart, LTi-like cells, were the first described ILC3s. These cells are CCR6⁺, produce IL-17A and IL-22 in response to PMA/Ionomycin or IL-23, and are required for the development of lymph nodes and gut-associated lymphoid tissue (Eberl et al, 2004; Takatori et al, 2009). LTi and LTi-like cells are subsetted into CD4⁺ (LTi₄) and CD4⁻ (LTi₀) populations, which are both able to produce IL-17A and IL-22 (Sawa et al, 2010). Both ROR γ ⁺ populations are represented in the adult mouse, but the frequency of LTi₀ cells in the fetus may be overestimated in cases where IL-7R α ⁺CD4⁻ markers, and not ROR γ ⁺, are used to identify these cells. Indeed, other IL-7R α ⁺CD4⁻ ILC populations besides LTi cells are present during development, as shown in Chapter 3.

In neonates, most LTi cells reside in developing PPs, while in the adult, LTi-like cells are additionally found in cryptopatches, lymphoid aggregates in the intestine that lack T and B cells. Cells at these two sites can be functionally divided by requirements for the aryl hydrocarbon receptor (AHR), a nuclear receptor activated by ligands supplied by diet (cruciferous vegetables), commensals, and endogenous molecules. AHR^{-/-} animals lack cryptopatches and isolated lymphoid follicles (ILFs), and have reduced frequencies of LTi₄ cells in lamina propria, while Peyer's patch development and the frequency of LTi₄ cells in PPs in adults remain unaffected (Lee et al, 2012). These data indicate that fetal LTi and adult LTi-like cells have different activities in the

intestine, and suggest that there are functional differences between cryptopatch and Peyer's patch populations in adults.

NK-22 cells are IL-15-independent ROR γ ⁺NKp46⁺CCR6⁻ cells that produce IL-22, but not IL-17A, in response to IL-23 (Cella et al, 2009). Like adult LTI-like cells, these cells are dependent on AHR, since NK-22 cells are absent in *Ahr*^{-/-} animals (Lee et al, 2012). However, germ free mice, and mice fed special diets that lack cruciferous vegetable-based ligands, still develop NK-22 cells that produce IL-22, suggesting that endogenous or yet unknown exogenous factors serve as ligands for AHR. NK-22 cells are found in the human, where they express NKp44 and are CCR6⁻ (Cella et al, 2009). Finally, the subset of NKp46⁺IL-7R α ⁺ cells in the mouse that expresses T-bet and IFN γ (ex-ROR γ cells) is covered in the section on ILC1s.

Development of innate lymphoid cells

IL-7R α ⁺ ILCs share a common precursor that is downstream of the common lymphoid progenitor. Two transcription factors, Id2 and PLZF, have been used to independently identify this precursor. Id2⁺ ILC precursors, which have been termed progenitors to all helper-like ILCs (CHILPs), are Lin⁻Id2⁺IL-7R α ⁺CD25⁻ α 4 β 7⁺flt3⁻ cells found in bone marrow and fetal liver (Klose et al, 2014). These cells do not express transcription factors associated with differentiated lineages, including ROR γ , T-bet, or Eomes, although they express intermediate levels of GATA3. Adoptively transferred bone marrow Id2⁺ ILC precursors into *Rag2/Il2rg* hosts differentiate into T-bet⁺ ILC1s, GATA3^{hi} ILC2s, and CCR6⁺ (CD4⁺ and CD4⁻) and CCR6⁻ (NKp46⁺ and NKp46⁻) ROR γ ⁺ ILC3s subsets, but not T, B, or cNK subsets. Similar results are found with adoptively transferred fetal liver Id2⁺ ILC precursors, although it is not clear whether ROR γ ⁺ and

ROR γ ^t NKp46⁺ cells are equally represented from fetal and adult-derived cells. Co-transfers of fetal and adult ILC precursors are required to formally test whether these populations preferentially give rise to different ILC populations.

A proportion of Id2⁺ ILC precursors in bone marrow express PLZF, a transcription factor expressed by NK T cells (Constantinides et al, 2014). Multiple T-bet⁺, GATA3^{hi}, and ROR γ ^t innate lymphoid populations lineage trace for PLZF, with the exception of CD4⁺ LTi-like cells. Additionally, CD4⁺ LTi-like cells do not develop from adoptively transferred PLZF⁺ bone marrow ILC precursors, although these precursors give rise to other IL-7R α ⁺ innate lymphoid lineages. These data suggest that LTi-like cells develop from ILC progenitors that precede the PLZF⁺ ILC precursor during development, although whether fetal LTi cells lineage trace for PLZF is unknown. These two studies together suggest that ILC precursors are a heterogeneous population, which include subsets with restricted lineage capacity.

Innate lymphoid cells and lymphoid organ development

Lymph nodes and Peyer's patches share requirements in the early stages of their development in the fetus. Lymphoid organogenesis in each case is induced by an initial wave of IL-7R α ⁺ROR γ ^tLT α ₁ β ₂⁺ LTi cells that activates LT β R⁺ stromal cells (lymphoid tissue organizers, or LTos) at sites that become the lymphoid organ anlage (Honda et al, 2001). Activated LTos express LTi-attracting chemokines, such as CXCL13 and CCL21, which recruit additional LTi cells to the anlage (Honda et al, 2001; Luther et al, 2003). This "second wave" of LTi cells further activates stromal cells at the developing site. Thus, *Lta*, *Ltb*, and *Ltbr*-deficient animals all have defects in lymphoid organ development, with most lymph nodes and Peyer's patches missing in animals that are

deficient in each of these genes (De Togni et al, 1994; Futterer et al, 1998; Koni et al, 1997). Also, animals that don't develop LTi cells, such as ROR γ ^{-/-} animals, do not develop secondary lymphoid tissue, indicating that this cell type is necessary for organogenesis (Eberl et al, 2004). In addition to lymphotoxin, LTi cells provide other required factors for lymphoid tissue development, since cross-linking of LT β R can rescue lymph node development in *Lta*-deficient mice, but not LTi-deficient ROR γ ^{-/-} animals. These factors are unknown, but are unlikely to include IL-22 since IL-22^{-/-} animals still develop lymphoid organs (De Luca et al, 2010; Kreymborg et al, 2007; Ota et al, 2011).

Major differences between lymph node and Peyer's patch development are the initial triggers that recruit the first LTi cells to the lymphoid tissue anlage. At lymph nodes, *Lta*-independent CXCL13 expressed by mesenchymal cells attracts LTi cells that first aggregate at the anlage by E13.5 (van de Pavert et al, 2009). This initial CXCL13 expression is activated by retinoic acid, a vitamin A metabolite. Retinoic acid induces CXCL13 in *Lta*^{-/-} mesenchymal cells in vitro, and retinoic acid-supplemented *Aldh1a2*^{-/-} embryos, which are unable to synthesize normal amounts of retinoic acid, do not express detectable CXCL13 at anlagen by E14.5. Thus, retinoic acid is critical for the first steps of lymph node organogenesis. At Peyer's patches, CD11c⁺ lymphoid tissue initiators (LTins) stimulated by RET ligands are proposed to initially activate the anlage, leading to the recruitment of the first wave of LTi cells (Veiga-Fernandes et al, 2007). In support of this model, diphtheria toxin-based killing of CD11c⁺ cells in CD11c-DTR mice leads to reduced Peyer's patch numbers even with incomplete depletion. CD11c⁺ cells express RET, and RET-deficient mice lack Peyer's patches despite having normal

frequencies of CD4⁺IL-7R α ⁺ LTi cells (Veiga-Fernandes et al, 2007). However, whether total numbers of LTi cells are reduced in RET-deficient animals due to defects in hematopoietic stem cells is unclear (Fonseca-Pereira et al, 2014). Determining whether LTi cell aggregation in the intestine is blocked after specific deletion of RET in CD11c⁺ cells would provide evidence that these factors work in the same pathway to activate stromal cells.

Since LTi cells are important for both the induction of lymphoid organ development as well as during the signal amplification phase, the numbers of LTi cells in tissue should modulate how these organs develop. Indeed, systems in which LTi numbers are altered in the intestine have shown differences in lymphoid organ number and size. In IL-7-overexpressing mice, increased numbers of LTi cells are associated with increased numbers of Peyer's patches and follicles per Peyer's patch (Meier et al, 2007). LTi₄ cell numbers are also regulated by retinoic acid, which promotes the development of these cells. Blocking retinoic acid signaling within hematopoietic cells decreases the frequency of LTi₄ cells in vivo, and is associated with smaller lymph nodes, reduced numbers of Peyer's patches, and fewer follicles per Peyer's patch (van de Pavert et al, 2014). In addition, pregnant mice that receive vitamin-A-deficient or vitamin-A high diets give birth to progeny that have smaller or larger lymphoid organs, respectively, in adulthood. Thus, alterations in lymphoid organ development during gestation have lasting effects on animals throughout life. These experiments suggest that LTi cells, and not LTin cells, determine the number of intestinal lymphoid organs that develop in the fetus, although it is possible that LTin and LTi cells are regulated by the same factors. Investigating how LTi cell numbers are modulated in the fetus before

and after lymphoid organ development is initiated will be important for determining how Peyer's patch size and numbers are determined.

Arginase

The enzyme arginase hydrolyses the conditionally essential amino acid L-arginine into L-ornithine and urea. Two isoforms of arginase have been described, arginase-1 (*Arg1*) and arginase-2 (*Arg2*). These enzymes are encoded by different genes, and are distinctly regulated in cellular expression. *Arg1* is located in chromosome 10 in mouse and chromosome 6 in human. Within cells, *Arg1* protein is located in the cytosol, and is responsible for completing the urea cycle in hepatocytes. The urea cycle, a series of biochemical reactions that removes excess nitrogen from blood by converting ammonia and bicarbonate into urea (Rothberg, 1958), allowed for the successful evolution of terrestrial, air-breathing animals by converting ammonia into a more neutral and water soluble compound that could be concentrated into small volumes of urine (Atkinson, 1992). *Arg1*-deficient mice are unable to remove ammonia from blood, and die between postnatal days 10-14 with high plasma levels of ammonia and arginine (Iyer et al, 2002). The second isoform, *Arg2*, is in chromosome 12 in mouse and chromosome 14 in human. *Arg2* protein is localized in mitochondria and is widely expressed in cells from nonhepatic tissues including the kidney and small intestine (Munder, 2009). *Arg2*-deficient mice are viable, and exhibit no obvious phenotype except for a 2-fold increase in plasma arginine in adult mice, highlighting the different functions between the two isoforms (Shi et al, 2001). *Arg2* has been proposed to be the ancestral gene, since the appearance of *Arg1* correlates with the evolution of vertebrates towards a terrestrial lifestyle (Srivastava & Ratha, 2010).

Arg1 is expressed by hematopoietic cells during infection and wound healing and has been proposed to have regulatory effects on inflammation and tissue remodeling during these processes (Munder, 2009). Immune cells that express Arg1 in the mouse are typically myeloid, with macrophages, dendritic cells, and granulocytes reported to express the enzyme after activation. In macrophages, Arg1 expression is induced by various stimuli. During helminth infection and allergic inflammation, IL-4 and IL-13 induce Arg1 expression by activating phosphorylation of STAT6. STAT6 dimers translocate to the nucleus and together with PU-1, C/EBP β , and the coactivator CREB binding protein, bind to an enhancer element upstream of the *Arg1* promoter (Pauleau et al, 2004). The STAT6-binding sequence of the enhancer element is required for IL-4/IL-13-dependent *Arg1* expression. Other mechanisms leading to the induction of Arg1 expression in macrophages are less characterized. Arg1 is induced in Mycobacteria-infected macrophages in a manner that is dependent on *Myd88* and partially affected by *Tlr2* deficiency, while being independent of *Stat6* (El Kasmi et al, 2008). More recently, Arg1 expression was reported in peritoneal macrophages that was dependent on GATA6 at rest and inducible with retinoic acid (Okabe & Medzhitov, 2014). Finally, lactic acid induces Arg1 in macrophages in a HIF1 α -dependent manner (Colegio et al, 2014). Thus, there are several pathways that lead to Arg1 induction in myeloid cells involving cytokines, metabolites, and pathogen-associated molecules.

Multiple mechanisms have been proposed as to how immune function is altered by arginase. L-ornithine, a product of arginine metabolism, can be further metabolized to produce polyamines, which may affect cell proliferation, and proline, a component of collagen. These molecules have been implicated in immune cell proliferation and

collagen remodeling in tissue, respectively. Importantly, L-arginine is also metabolized by nitric oxide synthase (NOS) to produce nitric oxide, a molecule that is toxic to cells and pathogenic organisms. As a competitive enzyme for L-arginine metabolism, arginase has been proposed to limit substrate availability for the synthesis of reactive nitrogen intermediates. Despite these proposed effects on immunity, there has been difficulty in finding requirements for Arg1 by myeloid cells in the lung during type 2 inflammation. Cellular infiltration, mucus and collagen production, and Th2 cytokine production are not altered by Arg1-deficiency in myeloid cells during chronic airway inflammation to *Schistosoma mansoni* eggs, ovalbumin, or *Aspergillus fumigatus* (Barron et al, 2013). However, there is evidence that Arg1 is important for immunity in the liver, since LysMcre/Arg1^{-flox} animals infected with *S. mansoni* by tail exposure die quicker than control mice, and have greater granulomatous inflammation and liver fibrosis (Pesce et al, 2009).

The advancement of tools to study Arg1 has opened the field to further investigation. Previously, arginase inhibitors such as NOHA or BEC were used to block Arg1 while bypassing the lethal effects of knocking out the *Arg1* gene (Tenu et al, 1999), but these inhibitors affect both arginase isoforms and may have widespread effects on liver and mitochondrial function. Now, using commercially available Arg1^{flox} animals, the Arg1 gene can be deleted in specific populations to study the in vivo functions of this enzyme in different cell types (El Kasmi et al, 2008). Also, the Arg1^{YFP} (YARG) reporter mouse allows for identification of additional cells that express Arg1 (Reese et al, 2007). In this thesis, the Arg1^{YFP} mouse was used extensively in chapters

2 and 3, in which I demonstrate that specific non-myeloid populations, including ILC1s, ILC2s, ILC3s, and ILC precursors, express Arg1.

Chapter Two:

Type 2 innate lymphoid cells constitutively express arginase-I in the naïve and inflamed lung

The text in this chapter has been published as: Bando JK, Nussbaum JC, Liang H-E, Locksley RM. Type 2 innate lymphoid cells constitutively express arginase-I in the naïve and inflamed lung (2013) *Journal of Leukocyte Biology*. 94(5):877-84 (2013)

Abstract

Arginase-I is produced by alternatively activated macrophages (AAMs) and is proposed to have a regulatory role during asthma and allergic inflammation. Here, we use an arginase-I-YFP (Yarg) reporter mouse to identify additional cellular sources of the enzyme in the lung. We demonstrate that type 2 innate lymphoid cells (ILC2s) express arginase-I at rest and during infection with the migratory helminth, *Nippostrongylus brasiliensis*. In contrast to AAMs, which express arginase-I following IL-4/IL-13-mediated STAT6 activation, ILC2s constitutively express the enzyme in a STAT6-independent manner. Although ILC2s deficient in the IL-33 receptor subunit T1/ST2 maintain arginase-I expression, IL-33 can regulate total lung arginase-I both by expanding the ILC2 population and by activating macrophages indirectly via STAT6. Finally, we find that ILC2 arginase-I does not mediate ILC2 accumulation, ILC2 production of IL-5 and IL-13, or collagen production during *N. brasiliensis* infection. Thus, ILC2s are a novel source of arginase-I in resting tissue and during allergic inflammation.

Introduction

Arginase-I is a urea cycle enzyme that hydrolyzes L-arginine into L-ornithine and urea (Morris, 2002). First identified in the mammalian liver, arginase-I is also highly induced during type 2 inflammation caused by allergens or parasites. Elevated arginase-I expression in lung tissue is observed in asthma models induced by sensitization with ovalbumin or *Aspergillus fumigatus*, as well as during helminth infection with *Nippostrongylus brasiliensis* larvae and *Schistosoma mansoni* eggs (Reece et al, 2006; Sandler et al, 2003; Zimmermann et al, 2003). Although arginase-I has been shown to suppress *S. mansoni*-induced fibrosis in the liver (Pesce et al, 2009), the functions of this enzyme in the lung during type 2 responses have been elusive (Barron et al, 2013).

Previous studies have demonstrated that macrophages activated by type 2 cytokines produce arginase-I during inflammation (Herbert et al, 2004; Hesse et al, 2001; Munder et al, 1998). Macrophages stimulated in this manner express a distinct set of genes in addition to arginase-I including chitinase 3-like 3 (*Chi3l3*)/Ym1, resistin-like alpha (*Retnla*)/Fizz1, and macrophage mannose receptor (MMR, *Mrc1*), and are designated alternatively activated in contrast to macrophages classically activated by IFN γ (Nair et al, 2003; Stein et al, 1992; Welch et al, 2002). Components of the IL-4/IL-13 signaling pathway required for alternative activation include IL-4R α , which complexes with the common gamma chain or IL-13R α 1 to form the IL-4R and IL-13R, respectively (Herbert et al, 2004), and STAT6, which is phosphorylated by IL-4R- and IL-13R-associated kinases and directly activates arginase-I gene expression (Pauleau et al, 2004; Rutschman et al, 2001). Although macrophages constitute a significant

source of arginase-I during type 2 inflammation, additional cellular sources of this enzyme have not been defined.

Type 2 innate lymphoid cells (ILC2s) are recently discovered cells that accumulate in tissue during type 2 inflammation, where they are important sources of IL-5 and IL-13 (Moro et al, 2010; Neill et al, 2010; Price et al, 2010). ILC2s are characterized as lineage-negative cells that express IL-7R α and T1/ST2, a component of the IL-33 receptor (Moro et al, 2010; Neill et al, 2010). Exogenous IL-33 increases ILC2 numbers, and T1/ST2-deficient mice have reduced ILC2s during inflammation, suggesting that IL-33 is critical for the expansion of this population (Neill et al, 2010; Price et al, 2010). The epithelial cytokines TSLP and IL-25 have additionally been shown to be important in ILC2 responses (Halim et al, 2012; Neill et al, 2010). Further understanding of ILC2 signaling and activation is needed to identify other functions of these cells during homeostasis and inflammation.

In this study, we characterize leukocyte populations that express arginase-I in the lung both at rest and during infection with the helminth *N. brasiliensis*. We show that ILC2s are a previously undescribed source of arginase-I in the lung, and that these cells express arginase-I independently of STAT6. We determine that IL-33 can regulate arginase activity in the lung both by increasing ILC2 numbers and by activating macrophages indirectly through cytokine-mediated STAT6 activation. Thus, arginase-I is regulated by STAT6-dependent and –independent pathways in discrete hematopoietic populations during type 2 inflammation.

Results

*Arginase-I is expressed by type 2 innate lymphoid cells and alternatively activated macrophages in the lung during *N. brasiliensis* infection*

To characterize hematopoietic populations that express arginase-I, we generated Arg1-YFP reporter mice, in which IRES-eYFP was inserted in exon 8 downstream of the endogenous stop codon and upstream of the 3' untranslated region (Reese et al, 2007). This insertion does not disrupt arginase-I expression as determined by enzyme assays conducted on tissue isolated from homozygous mice (data not shown). To induce type 2 inflammation, Arg1-YFP mice were infected subcutaneously with *N. brasiliensis*, which migrates through the lung within the first few days of infection (Camberis et al, 2003). Worms translocate to the intestine by day 3, but lung inflammation continues to intensify through 9-10 days post-infection (Voehringer et al, 2004).

On day 9, two major YFP⁺ populations were detected in the lung, which could be distinguished on the basis of CD11b expression (Fig 1a). YFP⁺ CD11b⁺ cells were macrophages based on expression of F4/80, MHC class II, and high autofluorescence (Fig 1b). These cells were also CD11c⁺ and Siglec-F⁺, consistent with their identification as alveolar macrophages. In contrast, the YFP⁺CD11b⁻ population lacked autofluorescence as well as the myeloid and lymphoid lineage markers CD11c, CD3, B220, and NK1.1 (Fig 1c and data not shown). We identified these lineage⁻ cells as ILC2s based on their expression of IL-7R α , T1/ST2, ICOS, KLRG1, and CD25. Over 90% of all T1/ST2⁺ ILC2s expressed YFP, making arginase-I an unexpected marker of ILC2s in the inflamed lung (Fig 1d).

To verify that ILC2s express arginase in wild-type mice, an enzyme assay was conducted to quantify urea production in lysates of cells sorted from the lungs of

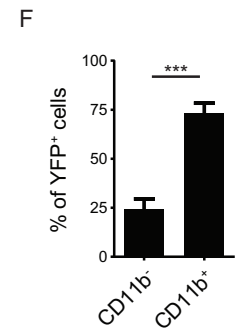
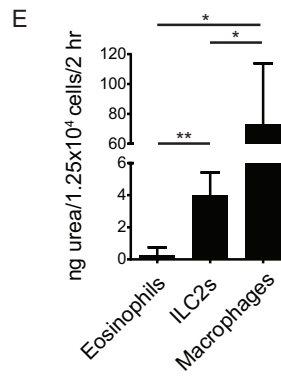
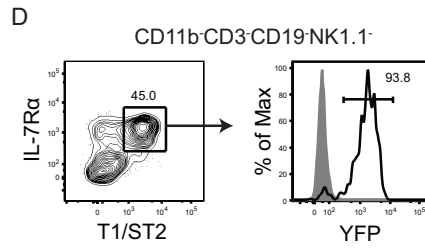
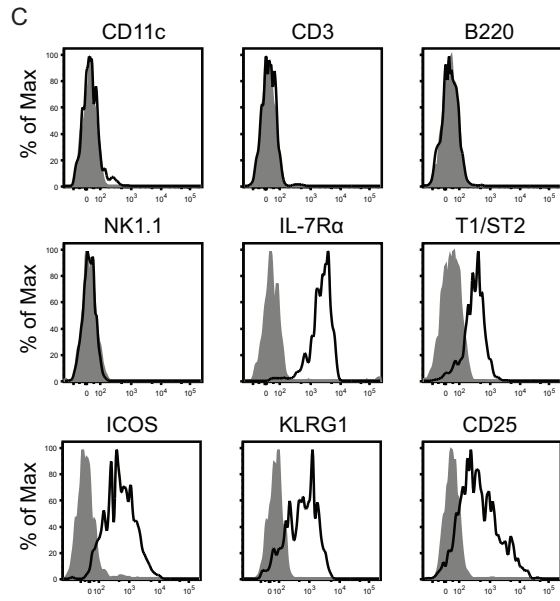
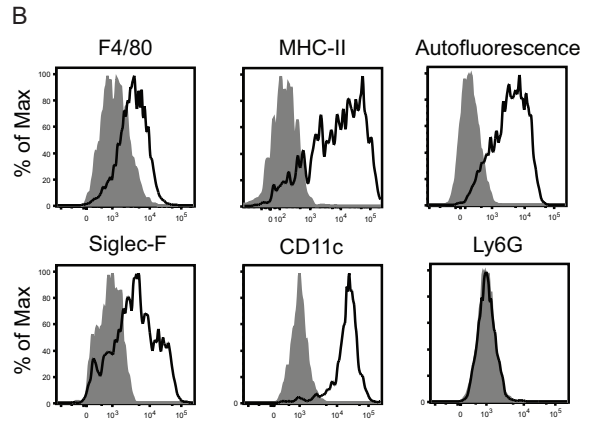
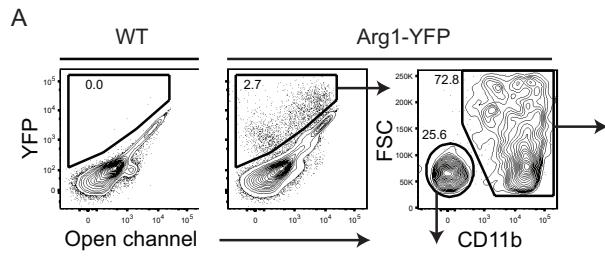


Figure 1. *Arginase-I* is expressed by type 2 innate lymphoid cells and alternatively activated macrophages in the lung during *N. brasiliensis* infection

(A) Flow cytometric analysis of YFP expression at day 9 of *N. brasiliensis* infection in Arg1-YFP mouse lungs. A wild-type control was used to set gates (left plot) and an open channel was used to identify autofluorescence. CD11b expression in YFP⁺ cells is shown in the right plot.

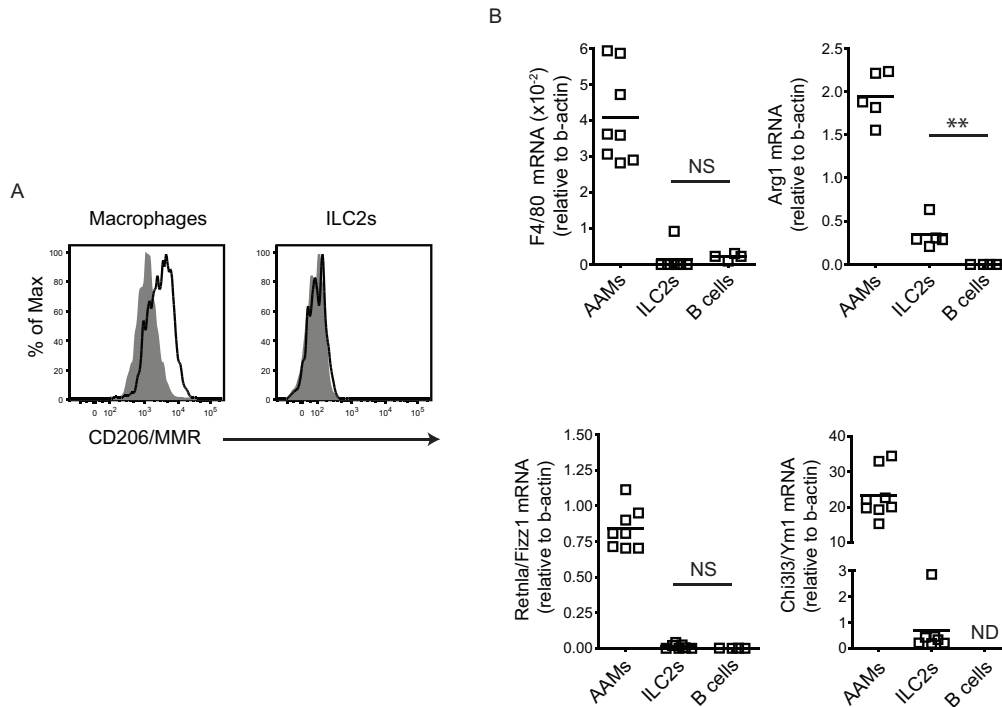
(B) Characterization of cell surface markers expressed by YFP⁺CD11b⁺ cells by flow cytometry. Shaded histograms represent isotype controls except in the histogram depicting autofluorescence, where the shaded plot represents autofluorescence in lymphocytes.

(C) Cell surface markers expressed by YFP⁺CD11b⁻ cells determined by flow cytometry. Shaded histograms are isotype controls.

(D) Expression of YFP in Lin⁻IL-7R α ⁺T1/ST2⁺ ILC2s. Cells were previously gated on live CD11b⁻CD3⁻CD19⁻NK1.1⁻ cells. The shaded histogram is from a wild-type control.

(E) Arginase enzyme assay in sorted lung populations from infected C57BL/6 mice. 1.25×10^4 cells of each population were sorted from day 12 infected lungs, lysed, and assayed for urea production in a 2 hr reaction in the presence of arginine. Data are representative of 2 independent experiments. n=4-5 mice per group, with samples from each mouse individually sorted. *p \leq 0.05, **p \leq 0.01.

(F) Percent of YFP⁺ cells that are CD11b⁻ (ILC2s) or CD11b⁺ (macrophages). n=6, pooled from 2 independent experiments ****p \leq 0.0001.



Supplementary Figure 1. *Assessment of AAM marker expression by ILC2s*

(A) Expression of CD206/macrophage mannose receptor by macrophages (F4/80⁺autofluorescent⁺) or ILC2s (Lin⁻IL-7R α ⁺T1/ST2⁺) in day 10-infected C57BL/6 lungs. Shaded histograms indicate isotype controls. Rat anti-mouse CD206 (MR5D3) antibodies were purchased from AbD Serotec.

(B) Relative expression of Arg1, Retnla/FIZZ1 and Chi3l3/Ym1 mRNA in lung AAMs (YFP+CD11b⁺), lung ILC2s (YFP+CD11b⁻), and splenic B cells sorted from day 10-infected Arg1-YFP mice. Relative expression of Emr1 (F4/80) mRNA is shown to demonstrate that sorted ILC2s samples did not contain AAMs. n=4-8, with each symbol representing a sort from an individual animal. **p \leq 0.01. Primer sequences were Actb forward 5'-GTG ACG TTG ACA TCC GTA AAG A-3' and reverse 5'-GCC GGA CTC ATC GTA CTC C-3' (ID: 145966868c1); Emr1 forward 5'-TGA CTC ACC TTG TGG TCC TAA-3' and reverse 5'-CTT CCC AGA ATC CAG TCT TTC C-3' (ID: 2078508a1); Arg1 forward 5'-CTC CAA GCC AAA GTC CTT AGA G-3' and reverse 5'-AGG AGC TGT CAT TAG GGA CAT C-3' (ID: 158966684c1); Retnla forward 5'-CCA ATC CAG CTA ACT ATC CCT CC-3' and reverse 5'-ACC CAG TAG CAG TCA TCC CA-3' (ID: 10048446a1); and Chi3l3 forward 5'-CAG GTC TGG CAA TTC TTC TGA A-3' and reverse 5'-GTC TTG CTC ATG TGT GTA AGT GA-3' (ID: 6753416a1). All sequences were selected from PrimerBank (Massachusetts General Hospital, Boston, MA).

infected C57BL/6 mice. Arginase enzyme activity was detected in ILC2 (Lin⁻IL-7R α ⁺T1/ST2⁺) and macrophage (CD11b⁺autofluorescent^{hi}), but not eosinophil cell lysates, validating our findings with the reporter mouse (Fig 1e). Based on enzyme activity, macrophages produced over 10-fold more arginase per cell than ILC2s. Arginase-I⁺ macrophages were also more abundant than ILC2s, which comprised about 25% of all arginase-I⁺ cells (Fig 1f).

To determine whether ILC2s shared other markers expressed by alternative activated macrophages, cells were assessed for expression of MMR, *Retnla*/FIZZ1, and *Chi3l3*/Ym1. ILC2s did not express MMR as assessed by flow cytometry, or *Retnla* mRNA as determined by q-PCR (S1a, b). *Chi3l3* mRNA was detected in ILC2s, and not in B cells, although expression levels of *Chi3l3* by ILC2s was low in comparison to AAMs; the difference in *Chi3l3* expression between AAMs and ILC2s was 48-fold, in comparison to the 6-fold difference in *Arg1* expression between the two populations. Thus, ILC2s express arginase-I without activating other components of the traditional transcriptional program associated with alternative activation in macrophages, with the possible exception of *Chi3l3*.

Type 2 innate lymphoid cells constitutively express arginase-I

The IL-4/IL-13/STAT6 signaling pathway induces alternatively activated genes, including *Arg1*, in macrophages (Herbert et al, 2004; Hesse et al, 2001; Munder et al, 1998; Pauleau et al, 2004; Rutschman et al, 2001). Because lung ILC2s express the receptor subunits IL-4R α , CD132 (common gamma chain), and IL-13R α 1, these cells have the potential to respond to IL-4 and IL-13 (Fig 2a). We investigated whether

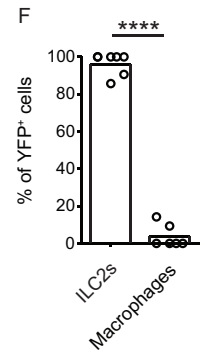
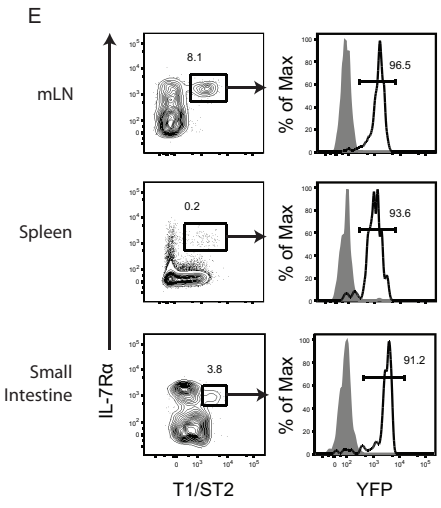
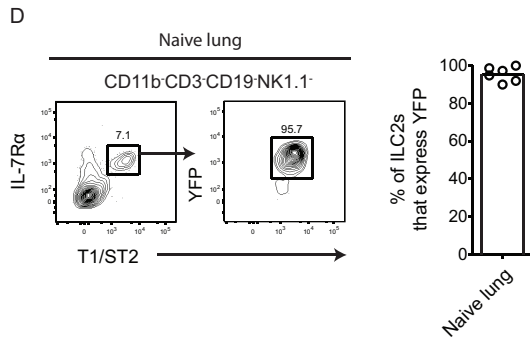
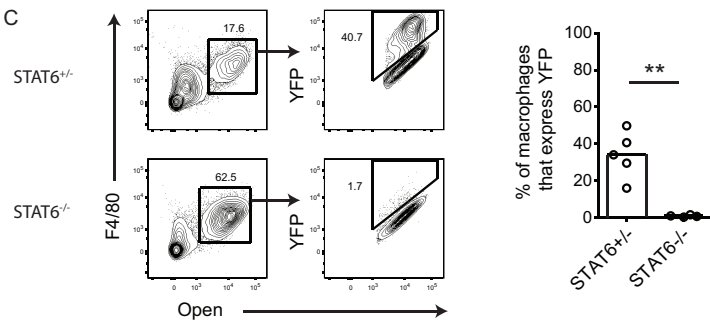
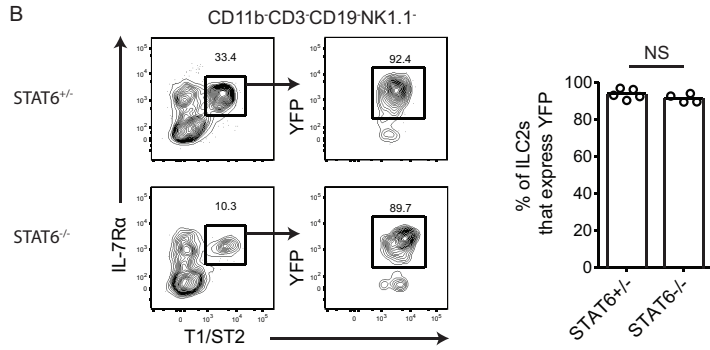
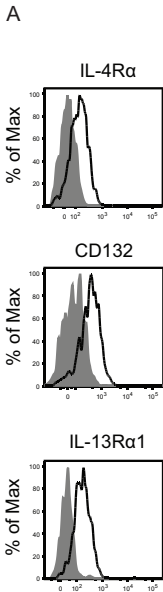


Figure 2. *Type 2 innate lymphoid cells constitutively express arginase-I*

(A) Expression of receptor subunits for type I and type II IL-4R in Lin⁻IL-7R α ⁺T1/ST2⁺ ILC2s by flow cytometry. Mice were infected with *N. brasiliensis* and lung cells were stained on day 9. Shaded histograms represent isotype controls.

(B) YFP expression in lung ILC2s and (C) macrophages in STAT6-deficient mice. Cells were obtained from *N. brasiliensis* infected lungs on day 9. Flow cytometry plots on the left show the gating scheme used to obtain percentages graphed in the right panel. ILC2 plots were previously gated on live CD11b⁻CD3⁻CD19⁻NK1.1⁻ cells. Data are representative of 2 independent experiments. n=4-5, **p \leq 0.01.

(D) YFP expression in ILC2s isolated from the lungs of naïve mice. Plots were previously gated on live CD11b⁻CD3⁻CD19⁻NK1.1⁻ cells. n=6, pooled from 2 independent experiments.

(E) YFP expression in Lin⁻IL-7R α ⁺T1/ST2⁺ cells from the mesenteric lymph nodes (mLN), spleen, and small intestine of naïve mice. Plots were previously gated on CD11b⁻CD3⁻CD19⁻NK1.1⁻ cells for the mesenteric lymph nodes, and CD11b⁻CD3⁻CD5⁻CD19⁻NK1.1⁻ cells for the spleen and small intestine.

(F) Percent of YFP⁺ cells that are ILC2s or macrophages in the naïve lung. n=6, pooled from 2 independent experiments. ****p \leq 0.0001

arginase-I expression by ILC2s was induced by IL-4/IL-13/STAT6 signaling by crossing arginase-I reporter mice with STAT6-deficient mice. Interestingly, Lin⁻IL-7R α ⁺T1/ST2⁺ lung ILC2s isolated from STAT6-deficient mice at 10 days post infection (dpi) maintained arginase-I expression (Fig 2b). In contrast, the percentage of F4/80⁺ autofluorescent macrophages that expressed arginase-I was reduced by >30-fold in infected STAT6 knock-out mice (Fig 2c).

Since arginase-I expression in ILC2s was not induced by STAT6 signaling, we investigated whether naïve ILC2s expressed the enzyme at rest. Indeed, >90% of ILC2s isolated from the naïve lung, mesenteric lymph nodes, spleen, and small intestine expressed arginase-I, indicating that ILC2s express the enzyme constitutively (Fig 2d, e). In the uninfected lung, ILC2s comprised over 90% of all arginase-I⁺ cells (Fig 2f), making this population the primary hematopoietic cell source of arginase-I in the resting lung.

Arginase-I deficiency does not affect ILC2 numbers or cytokine production

We next investigated whether arginase-I expression is required for ILC2 accumulation or function. Arginase-I-deficiency in mice is fatal two weeks after birth due to loss of the enzyme in hepatic cells (Iyer et al, 2002). To circumvent this issue, arginase-I floxed (Arg1-flox) mice have been generated to facilitate deletion of the enzyme in specific cell types of interest (El Kasmi et al, 2008). To target arginase-I deletion to ILC2s, we used Red5 mice, in which the IL-5 locus is disrupted by a construct containing RFP-IRES-Cre recombinase (Molofsky et al, 2013). In these mice, ILC2s, but not macrophages, express RFP and Cre in *N. brasiliensis*-infected lungs as

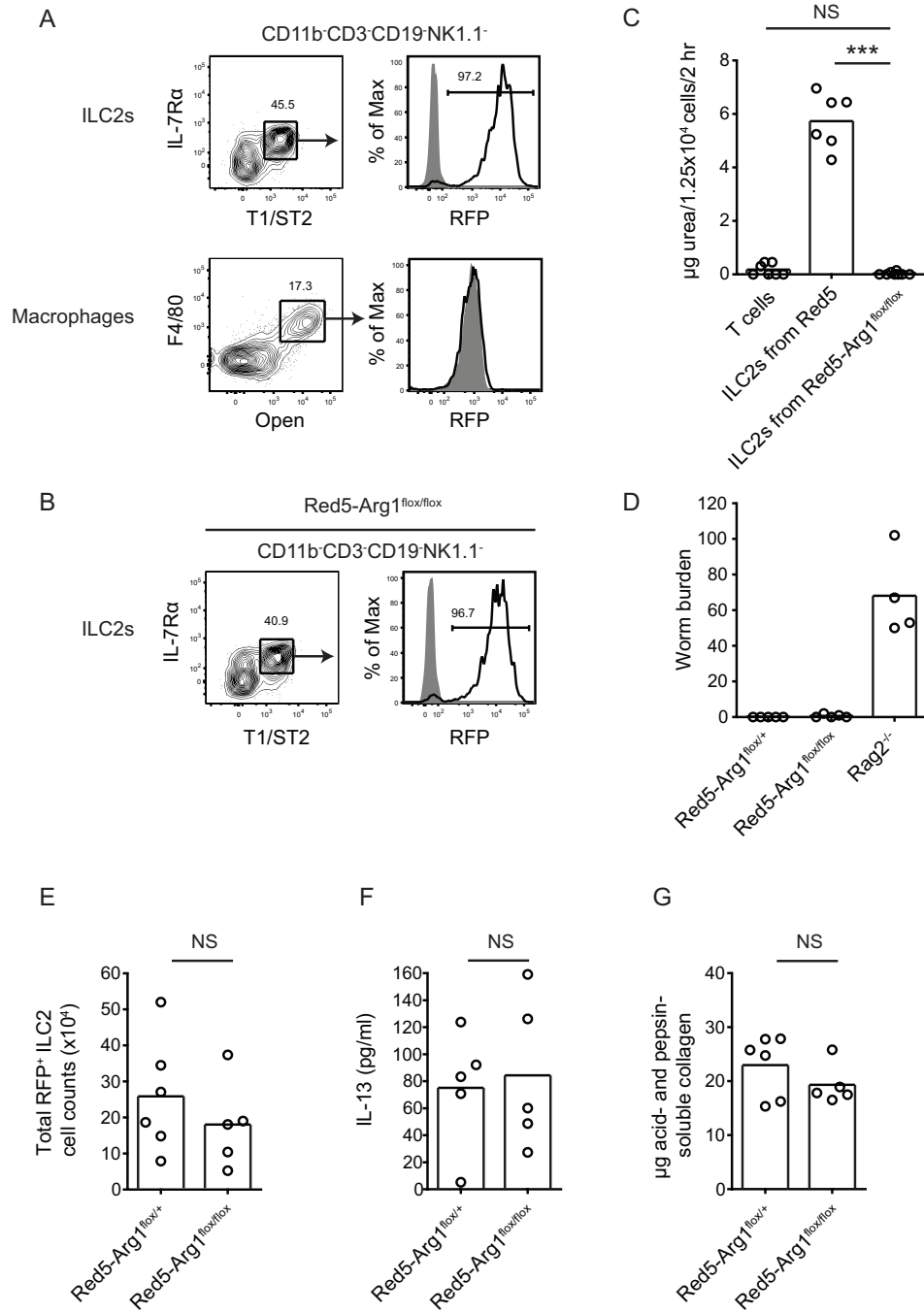


Figure 3. *Arginase-I* deficiency does not affect ILC2 numbers or cytokine production

(A) RFP expression in ILC2s (top plots) or macrophages (bottom plots) in Red5 lungs on day 10 of *N. brasiliensis* infection. The shaded histograms represent wild-type controls. Plots for ILC2s were previously gated on live CD11b⁻CD3⁻CD19⁻NK1.1⁻ cells.

(B) RFP expression in ILC2s from Red5-Arg1^{flox/flox} lungs at day 10 of infection. The shaded histogram represents a wild-type control. Plots were previously gated on live CD11b⁻CD3⁻CD19⁻NK1.1⁻ cells.

(C) Arginase enzyme assay in ILC2s sorted from Red5-Arg1^{flox/flox} lungs. 1.25×10^4 Lin⁻IL-7R α ⁺T1/ST2⁺ cells or CD4⁺ T cells were sorted from lungs at day 10 of *N. brasiliensis* infection, lysed, and assayed for urea production over a 2 hr reaction in the presence of arginine. n=6, pooled from 2 independent experiments, with each n being a sort from an individual mouse. ***p \leq 0.001

(D) Worm burden in Red5-Arg1^{flox/flox}, Red5-Arg1^{flox/+}, and Rag2^{-/-} positive controls at day 10 of infection. Data are representative of 2 independent experiments. n=4-5.

(E) Total lung RFP⁺ ILC2 counts in Red5-Arg1^{flox/flox} mice compared to Red5-Arg1^{flox/+} controls at day 10 of infection. Data are representative of 3 independent experiments. n=5-6

(F) IL-13 detected in the supernatants of unstimulated cultures of ILC2s. ILC2s were sorted from day 10-infected mouse lungs and incubated in complete RPMI for 8 hr. Data are representative of 2 independent experiments. n=5.

(G) Assessment of uncrosslinked collagen in Red5-Arg1^{flox/flox} mice at day 10 of infection. Acid- and pepsin- soluble collagen was extracted from the right superior lobe of the lung. Data are representative of 2 independent experiments. n=5-6.

detected by flow cytometry (Fig 3a). We crossed Red5 mice with Arg1-flox mice to generate Red5-Arg1^{flox/flox} mice, in which cells expressing IL-5 activate the recombinase and delete the *Arg1* gene. Red5-Arg1^{flox/flox} mice were healthy and had no obvious abnormalities (data not shown).

In *N. brasiliensis*-infected Red5-Arg1^{flox/flox} mice, the percentage of the ILC2 population that expressed RFP was similar to that seen in Red5 mice, indicating that there was no selective growth advantage in rare Red5-negative cells (Fig 3b). ILC2 lysates from these mice were deficient in arginase activity as assayed by urea production, indicating successful deletion of the *Arg1* gene (Fig 3c). The lack of enzyme activity in arginase-I-deficient ILC2s also demonstrated that mitochondrial arginase-II does not compensate for the absence of arginase-I in these cells.

Red5-Arg1^{flox/flox} mice cleared worms normally by day 10 of infection (Fig 3d). At this time point, equivalent numbers of IL-5-producing ILC2s were present in infected Red5-Arg1^{flox/flox} lungs as compared to Red5-Arg1^{flox/+} controls based on RFP⁺ cell counts (Fig 3e). The MFI of RFP also was unchanged by arginase-I deficiency (3a, b, and data not shown). To assay other cytokines, ILC2s were sorted from infected lungs and cultured without stimulation. After 8 hr, supernatants from arginase-I-deficient and -sufficient ILC2 cultures contained equivalent amounts of IL-13, while IL-9 was undetectable in all cultures (Fig 3f and data not shown). Thus, arginase-I does not influence the accumulation of cytokine-producing ILC2s in the lung during worm infection.

To assay collagen production, infected lungs were digested overnight with pepsin and acetic acid to solubilize uncrosslinked collagen. There was no difference in the

amounts of acid- and pepsin- soluble collagen extracted from Red5-Arg1^{flox/flox} lungs and Red5-Arg1^{flox/+} controls, indicating that loss of ILC2-derived arginase-I does not affect collagen production during *N. brasiliensis* infection (Fig 3g).

IL-33 can regulate arginase-I⁺ cell numbers in lung tissue

IL-33, a member of the IL-1 superfamily of cytokines, has been implicated in the activation and expansion of ILC2s (Moro et al, 2010; Neill et al, 2010; Price et al, 2010). We reasoned that IL-33 could alter arginase-I expression in the lung by regulating ILC2 cell numbers. We first investigated whether arginase-I expression in ILC2s was affected by IL-33R deficiency using T1/ST2^{-/-} mice. This deficiency precludes the use of T1/ST2 as a marker of ILC2s, so this population was identified as Lin⁻IL-7R α ⁺CD25⁺ (Fig 4a). Based on these markers, ILC2s continue to express arginase-I in the absence of IL-33R (Fig 4a, b), providing additional evidence for constitutive expression of this enzyme. As expected, there were significantly fewer CD11b⁻ arginase-I⁺ cells (ILC2s) in T1/ST2^{-/-} lungs compared to wild-type controls on day 9 of infection (Fig 4c).

To test whether IL-33 is sufficient to increase arginase-I expression in the lung by expanding ILC2s, recombinant IL-33 was administered to wild-type Arg1-YFP mice intranasally for three days. On day four, there were higher numbers of both arginase-I⁺ ILC2s and macrophages in the lung following IL-33 treatment (Fig 4d). Since IL-33 can induce the production of type 2 cytokines, we investigated whether the increase in the numbers of these two arginase-I⁺ cell types was due to IL-4/IL-13 signaling. In STAT6-deficient mice treated with recombinant IL-33, arginase-I expression by macrophages was significantly abrogated (Fig 4d). In contrast, arginase-I⁺ ILC2 numbers remained

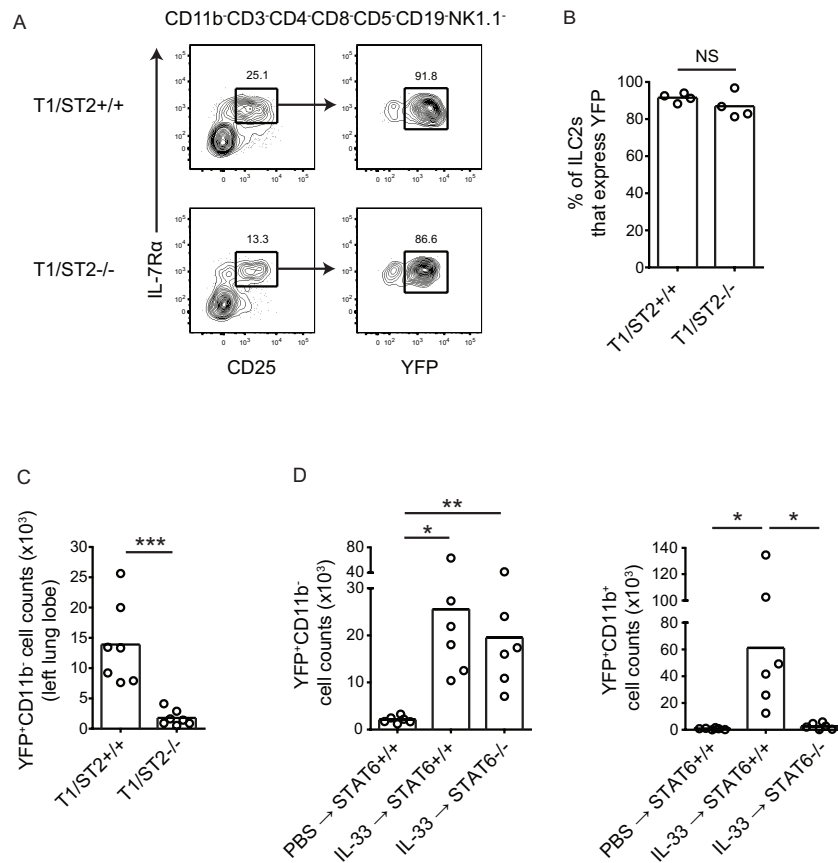


Figure 4. *IL-33 can regulate arginase-1⁺ cell numbers in lung tissue*

(A) Identification of ILC2s in T1/ST2-deficient mouse lungs using IL-7R α and CD25. Cells are from day 9 of *N. brasiliensis* infection.

(B) Percent of lung ILC2s that express YFP in T1/ST2-deficient mice during inflammation. Cells were isolated from the left lung lobe at day 9 of *N. brasiliensis* infection. n=4

(C) Total lung YFP⁺CD11b⁻ (ILC2) cell counts from infected T1/ST2-deficient mice. Cell counts are from the left lung lobe at day 9 of *N. brasiliensis* infection. Data are pooled from 2 independent experiments. n=7, ***p \leq 0.001.

(D) Total lung YFP⁺CD11b⁻ (ILC2) and YFP⁺CD11b⁺ (alternatively activated macrophage) cell counts after administration of intranasal IL-33 in STAT6-deficient and -sufficient mice. 500 ng IL-33 was administered daily for 3 days, and cell counts in the whole lung were determined on day 4. n=6, and are the pooled data from 2 independent experiments. *p \leq 0.05, **p \leq 0.01

elevated even in the absence of STAT6 signaling. These data demonstrate that IL-33 can increase lung arginase-I in two ways: by STAT6-independent expansion of the pool of constitutively arginase-I⁺ ILC2s and by induction of IL-4/IL-13 leading to STAT6-dependent alternative macrophage activation.

Discussion

Elevated arginase-I expression has been observed in the lung during type 2 inflammation, but a thorough survey of the cells responsible for producing this enzyme has not been performed. In this study, we used an arginase-I reporter mouse to identify cells that express this enzyme *in vivo*, and determined that both macrophages and ILC2s express arginase-I in the lung during helminth infection. Although our data confirm prior findings that alternatively activated macrophages are the predominant source of arginase-I in the *N. brasiliensis*-infected lung based on abundance and enzyme activity per cell (Reece et al, 2006), we identify ILC2s as the primary hematopoietic source of arginase-I under resting conditions.

Our identification of ILC2s was based on cell surface markers (IL-7R α , T1/ST2, ICOS, and CD25) and FSC/SSC characteristics widely used to describe IL-5-or IL-13-producing lineage-negative cells. Based on these markers, over 90% of ILC2s express arginase-I in both the resting and infected lung, making this enzyme a consistent marker for lung ILC2s. Thus, the Arg1-YFP reporter mouse will be a useful tool for identifying lung ILC2s in future studies. Although we demonstrated that ILC2s expressed arginase-I in other organs, including the mesenteric lymph node, spleen, and small intestine, the full characterization of cell populations that express arginase-I in these tissues remains to be determined. Still, *Arg1*, in combination with other ILC2 genes, may be useful to

genetically target these cells without relying on cytokine production for identification.

The discovery of new markers for ILC2s remains important, since there are few known ILC2 genes that are distinct from those expressed by T cell subsets.

In this study, we used STAT6-deficient mice to establish that the IL-4/IL-13/STAT6 signaling pathway is not required for arginase-I expression in ILC2s. It remains to be determined how *Arg1* transcription is regulated in ILC2s. STAT6-independent mechanisms that induce arginase-I exist in macrophages, although they have not been described during type 2 inflammatory responses. During *Mycobacterium bovis* infection, arginase-I is regulated by MyD88 and the transcription factor C/EBP β , which binds to an enhancer upstream of *Arg1* and can regulate gene expression in the absence of STAT6 (El Kasmi et al, 2008). Although it is unlikely that MyD88 signaling activates arginase-I expression in ILC2s due to the constitutive expression of this enzyme in naïve and T1/ST2 KO mice, involvement of C/EBP β in ILC2 arginase-I expression will require further investigation. Future studies determining whether the constitutive expression of arginase-I is established during ILC2 development may lead to insights as to how expression of arginase-I is controlled.

IL-33 has been shown to be an important factor in the activation and expansion of ILC2s. Here, we demonstrate that IL-33 can enhance the expression of arginase-I in the lung by expanding the size of the ILC2 compartment but not the level of arginase-I expression per cell. We anticipate that other cytokines that expand ILC2 numbers, such as TSLP and IL-25, will also increase arginase-I expression in the lung by this mechanism. Since IL-33, TSLP, and IL-25 are implicated in the initiation of type 2 responses, we speculate that ILC2 recruitment and expansion may represent a rapid

mechanism for increasing arginase activity in tissue. Experiments examining the kinetics of ILC2 numbers and macrophage activation after different types of stimuli and in additional tissues will elucidate this further.

The two pathways that serve to enhance arginase-I expression in the lung during type 2 inflammation suggest that this enzyme has important roles in this tissue. Despite this, the function of arginase-I in the lung has been elusive. Our data using mice deficient in arginase-I specifically in ILC2s indicate that arginase-I expression does not affect ILC2 numbers or cytokine production in the lung after worm infection. However, arginase-I was deleted in cells that produce IL-5, and therefore we cannot exclude a role for the enzyme early in ILC2 development or differentiation. Future studies targeting arginase-I expression using alternative strategies in ILCs may shed light on additional functions of these cells and their enzymatic activities.

We speculate that the effects of arginase-I expression by ILC2s will be seen more prominently in environments where AAMs are absent. ILC2s are present in naïve mice, and thus it will be of interest to study whether enzyme production by this cell type is important for maintenance of tissue homeostasis. The immune and metabolic functions of arginase-I expression by ILC2s in various tissues in naïve and infected mice remain intriguing areas for investigation.

Materials and Methods

Mice

Arg1-YFP (also called YFP-Arg1, or Yarg) mice were previously described (Reese et al, 2007). Red5 mice contain an RFP-IRES-Cre recombinase construct that replaces the endogenous *IL5* gene as described (Molofsky et al, 2013). STAT6^{-/-} mice and Arg1-flox mice were purchased from Jackson Laboratories (Bar Harbor, ME) (El Kasmi et al, 2008; Kaplan et al, 1996). T1/ST2-deficient mice (a generous gift from M. Steinhoff, University of California, San Francisco, CA) have been described (Hoshino et al, 1999). All mice were backcrossed to C57BL/6 for at least 10 generations. Studies were conducted in accordance with the UCSF Institutional Animal Care and Use Committee.

Tissue dissociation

Lungs were perfused with 10 ml PBS, removed, minced, and pressed through a 70 µm nylon mesh to obtain a single-cell suspension. Small intestines were digested in 0.1 Wunsch/ml Liberase TM (Roche Applied Science, Indianapolis, IN) for 4 cycles of 20 min incubations and filtered through 70 µm nylon mesh. Hematopoietic intestinal cells were enriched by Percoll density gradient separation.

Flow cytometry

Rat anti-mouse CD3 (17A2), rat anti-mouse IL-7Rα (A7R34), rat anti-mouse F4/80 (BM8), rat anti-mouse Ly6G (RB6-8C5), mouse anti-mouse NK1.1 (PK136), rat anti-mouse MHC class II (M5/114.15.2) and rat anti-mouse IL-13Rα1 (13MOKA) antibodies and streptavidin APC were purchased from eBioscience (San Diego, CA); rat

anti-mouse CD11b (M1/70), Armenian hamster anti-mouse CD11c (HL3), rat anti-mouse CD132 (FCM), and rat anti-mouse Siglec-F (E50-2440) antibodies were purchased from BD Pharmingen (San Jose, CA); rat anti-mouse B220 (RA3-6B2), rat anti-mouse CD25 (PC61), Syrian hamster anti-mouse KLRG1 (2F1/KLRg1), and Armenian hamster anti-mouse ICOS (C398.4A) were purchased from Biolegend (San Diego, CA); and rat anti-mouse T1/ST2 (DJ8) antibodies were purchased from MD Bioproducts (St. Paul, MN).

Antibody-stained samples were incubated with DAPI and live cells were selected by gating on DAPI⁻ cells that had a cellular FSC/SSC profile. To gate on Arg1-YFP⁺ macrophages, an open channel was used (PE, PerCP-cy5.5 or AmCyan) to account for autofluorescence. Cell surface marker expression on macrophages, with the exception of Siglec-F, was determined using APC-conjugated antibodies, because macrophage autofluorescence was minimal in the APC channel. Autofluorescence histograms were determined by comparing macrophages to lymphocytes in the PerCP-cy5.5 channel. Cell counts were calculated using CountBright absolute counting beads (Invitrogen, Grand Island, NY). Flow cytometry experiments were done using a BD Biosciences LSR II with FACSDiva software. Data were analyzed with FlowJo (TreeStar, Ashland, OR).

Nippostrongylus brasiliensis infection

Mice were infected with *N. brasiliensis* as described (Voehringer et al, 2004). Briefly, mice were anesthetized with isoflurane and injected with 500 third stage larvae (L3) subcutaneously in 200 μ l saline. Mice were kept on antibiotic water (2 g/L neomycin sulfate, 100 mg/L Polymixin B) for the first 5 days post infection. Worm burden was

assessed in the small intestine by incubating filleted tissue in 10 ml of HBSS for 2 hr and counting worms under a dissecting microscope.

IL-33 treatment

Mice were anesthetized with isoflurane and given 500 ng of recombinant IL-33 (R&D, Minneapolis, MN) in 20 μ l PBS *i.n.* for three consecutive days. On the fourth day, whole lungs were isolated for flow cytometry.

Measurement of ILC2 cytokine production

1×10^4 Lin⁻IL-7R α ⁺T1/ST2⁺ ILC2s were sorted from infected lungs using a MoFlo XDP (Beckman Coulter, Brea, CA), and cells were incubated in 100 μ l of complete RPMI at 37°C. After 8 hr, supernatants were assayed for IL-9 and IL-13 by cytokine bead array (BD Biosciences).

Measurement of acid- and pepsin- soluble collagen

The superior lobes of infected mouse lungs were finely minced and incubated with 0.1 mg/ml pepsin (Sigma) in 0.5 M acetic acid overnight. Supernatants were neutralized and labeled with Sircol dye (Biocolor, UK).

Arginase enzyme activity assay

Eosinophils, ILC2s, and macrophages were sorted from C57BL/6 mice, and arginase enzyme activity was determined using a modified version of published methods (Corraliza et al, 1994). 2.5×10^4 cells from each population were lysed in 50 μ l of 0.1% Triton X-100 containing protease inhibitors (Complete Mini protease inhibitor cocktail, EDTA-free, Roche Applied Science, Indianapolis, IN), and incubated with 50 μ l

of 10 mM MnCl₄H₂O, 50 mM Tris-HCl, pH 7.5, for 10 min at 55°C to activate arginase. 50 µl aliquots were transferred to two Eppendorf tubes and mixed with 50 µl of 0.5 M arginine, pH 9.7 (Sigma, St. Louis, MO). Samples were either incubated for 2 hr at 37°C and then stopped with 400 µl of a 1:3:7 acid mixture of H₂SO₄, H₃PO₄, and H₂O, or were immediately stopped to establish urea production at time zero. 12.5 µl of 9% α-isonitrosopropiophenone (Sigma) dissolved in 100% ethanol were added to stopped samples and incubated at 95°C. ODs were read at 540 nm with a microplate reader (Molecular Devices, Sunnyvale, CA), and arginase enzyme activity was determined by subtracting the urea detected in samples at time zero from the urea detected after the two hr reaction.

Statistics

Data were analyzed using the two-tailed unpaired Student's t-test.

Acknowledgements

The authors thank Z. Wang for expertise in cell sorting.

Chapter Three:

Identification and distribution of ILC precursors in the fetal mouse intestine

The text in this chapter has been submitted as: Bando JK, Liang H-E, Locksley RM.
Identification and distribution of ILC precursors in the fetal mouse intestine.

Abstract

Fetal lymphoid tissue inducer (LTi) cells are required for lymph node and Peyer's patch (PP) organogenesis, but where these specialized group 3 innate lymphoid cells (ILC3s) develop remains unclear. Here, we identify extrahepatic arginase-1⁺, Id2⁺ ILC precursors in the fetus (fILCPs) that differentiate into ILC1s, ILC2s, and ILC3s. These precursors populate the intestine by E13.5, and prior to PP organogenesis (E14.5-E15), are broadly dispersed in the proximal gut, correlating with where PPs first develop. At E16.5, after PP development begins, fILCPs accumulate at PP anlagen in a lymphotoxin- α -dependent manner. Thus, fILCPs exit the liver and accumulate in the intestine, where they are recruited to the primordial PP by activated stromal cells and become a localized source of mature ILC populations.

Introduction

Peyer's patches (PPs) are aggregated lymphoid follicles in the small intestine that sample intestinal luminal antigens and facilitate mucosal immune responses. In the mouse, PP organogenesis is induced during fetal development by hematopoietic lineage $(Lin)^-c\text{-kit}^+IL\text{-}7R\alpha^+CD4^{+/-}ROR\gamma^t^+$ lymphoid tissue inducer (LTi) cells (Eberl et al, 2004; Yoshida et al, 1999). LTi cells induce PP development by activating lymphotoxin- β receptor (LT β R) signaling in stromal lymphoid tissue organizer (LTo) cells through expression of the LT β R ligand, LT $\alpha_1\beta_2$ (De Togni et al, 1994; Futterer et al, 1998; Honda et al, 2001; Koni et al, 1997). Activated LTo cells initiate a positive feedback loop by expressing chemokines that attract additional LTi cells to the anlage (Honda et al, 2001; Okuda et al, 2007). LTi cells are essential for secondary lymphoid tissue development, since LTi-deficient $ROR\gamma^t^{-/-}$ mice do not develop PPs or lymph nodes (Eberl et al, 2004).

LTi cells belong to a family of innate lymphoid cells (ILCs), which are dependent on common gamma chain (γ_c) cytokines for development, but lack common lineage markers and do not express somatically rearranged receptor genes dependent on recombination activating genes (*Rag1/Rag2*) (Spits & Cupedo, 2012). ILCs participate in a wide range of immune responses, and have been divided into groups based on transcription factor and cytokine expression. Group 1 ILCs (ILC1s) express the transcription factor T-bet and produce the cytokine IFN γ ; group 2 ILCs (ILC2s) express high levels of the transcription factor GATA3 and produce the cytokines IL-5 and IL-13; and group 3 ILCs (ILC3s), which include fetal LTi cells, express the transcription factor $ROR\gamma^t$ and produce the cytokines IL-22 and IL-17A. In contrast to other innate lymphoid

populations, LT_i cells are abundant in the fetal intestine and are the only described ILCs in the fetal mouse that function in organ development.

The development of LT_i cells and other ILCs is dependent on the E2A transcriptional inhibitor Id2, indicating a shared developmental pathway for ILC lineages (Moro et al, 2010; Satoh-Takayama et al, 2010; Yokota et al, 1999). Lin⁻Id2⁺α4β7⁺flt3⁻CD25⁻ ILC precursors have recently been identified in fetal liver and adult bone marrow (BM), the major sites of hematopoiesis in fetuses after embryonic day (E) 10.5 and adults, respectively (Klose et al, 2014). These cells have the capacity to differentiate into NK1.1⁺IL-7Rα⁺T-bet⁺ ILC1s, GATA3⁺ ILC2s, and RORγt⁺ ILC3s, but not T cells, B cells, or conventional NK cells. Id2⁺ ILC precursors in adult bone marrow (BM) express GATA3, but lack T-bet and RORγt. A subset of Id2⁺ ILC progenitors also expresses the transcription factor PLZF, another reported marker for ILC precursors in adult BM and fetal liver (Constantinides et al, 2014; Klose et al, 2014).

Although ILC precursors have been described at sites of hematopoiesis, little is known about these cells in peripheral tissues. In the fetal mouse, there is evidence that ILC precursors exist outside of the liver, since LT_i cells have been derived in vitro from Lin⁻c-kit⁺IL-7Rα⁺α4β7⁺RORγt^{GFP-} cells from the intestines of E14 RORγt^{GFP} 'knock in' reporter mice (Cherrier et al, 2012). Although these data suggest that undifferentiated ILC precursors can disperse into the fetal intestine and continue their development in tissue, the location and lineage potential of these extrahepatic ILC precursors remain unclear.

Arginase-I (Arg1) is a urea cycle enzyme that is induced in macrophages during type 2 immune responses and wound repair (Herbert et al, 2004; Hesse et al, 2001;

Munder et al, 1998; Sandler et al, 2003). We recently reported that Arg1 expression by hematopoietic cells is not confined to myeloid populations, but also occurs constitutively in ILC2s in adult mice (Bando et al, 2013). Here, we demonstrate that Arg1 is additionally expressed by fetal ILC precursors (fILCPs) and their progeny in the fetal intestine. Arg1⁺ intestinal fILCPs are capable of differentiating into ILC1, ILC2, and ILC3 populations. Additionally, we show that fILCPs are present in proximal portions of the fetal small intestine prior to PP development, and accumulate at the developing PP in a LT α -dependent manner once intestinal lymphoid tissue organogenesis is initiated. These results indicate that ILC precursors generate mature ILCs at developing peripheral lymphoid organs during fetal development.

Results:

Arginase-I expression marks LTi-like cells in the adult mouse intestine

We previously reported that ILC2s constitutively express Arg1, and that ILC2s are >95% of all Arg1-expressing hematopoietic cells in the naïve mouse lung (Bando et al, 2013). We next investigated Arg1 expression in the enteric system to determine whether additional cell populations express the enzyme. Using the Arg1^{YFP} reporter mouse, in which a construct containing IRES-YFP was inserted in exon 8 of the *Arg1* gene without disrupting enzyme expression (Reese et al, 2007), we determined that YFP⁺ cells made up less than 1% of hematopoietic cells isolated from the small intestine (lamina propria and intraepithelial cells combined) (Fig. 1A). These cells were identified as ILCs based on their expression of Thy1 and IL-7R α , and lack of common myeloid and lymphoid lineage surface markers CD11b, CD11c, CD3, B220, NK1.1 and NKp46

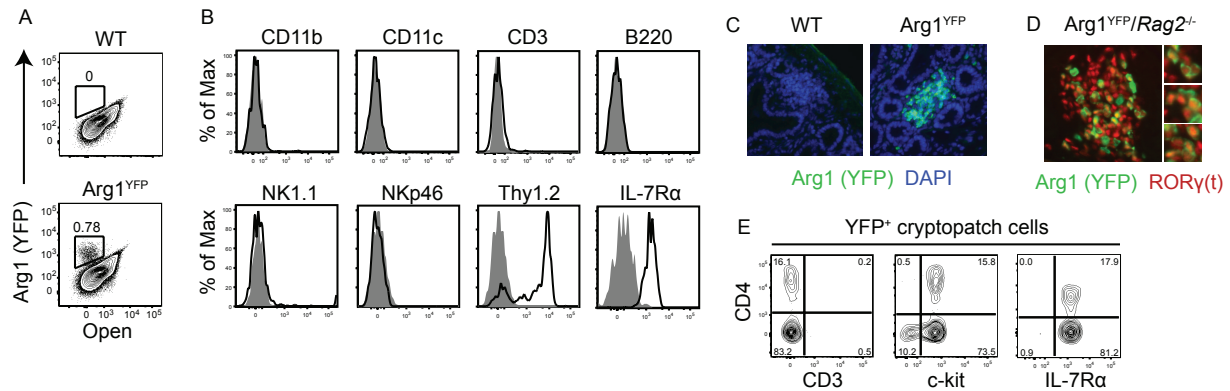


Figure 1. ***Arg1*** is expressed by *LTi*-like cells in cryptopatches.

(A) YFP⁺ cells in the small intestines of adult WT and Arg1^{YFP} mice. Plots show live CD45⁺ cells. (B) Surface markers expressed by YFP⁺ cells in the small intestine. (C) Histological sections of WT and Arg1^{YFP} cryptopatches. Sections are counterstained with DAPI. (D) Anti-mouse RORγ(t) antibody staining in an Arg1^{YFP}/Rag2^{-/-} cryptopatch. (E) Surface markers expressed by YFP⁺ cells isolated from dissected cryptopatches.

(Fig. 1B). Unexpectedly, in wild type and *Rag2*^{-/-} mice, intestinal Arg1-expressing cells were present in cryptopatches (Fig. 1C, D), tertiary lymphoid structures that contain LTi-like cells and CD11c⁺ dendritic cells (Eberl & Littman, 2004; Kanamori et al, 1996). To test whether YFP⁺ cells expressed LTi-like cell surface markers, cryptopatches were dissected from the small intestine and analyzed by flow cytometry. YFP⁺ cells isolated from cryptopatches were IL-7Rα⁺c-kit⁺CD4^{+/-}CD3⁻, consistent with the profile of LTi-like cells (Fig. 1E). Furthermore, YFP⁺ cells in cryptopatches expressed the LTi transcription factor RORγt as determined by RORγ(t) antibody staining in *Rag2*^{-/-} mice (Fig. 1D). RORγt⁺ cells that did not express Arg1 were also present in cryptopatches, indicating that heterogeneity exists among cryptopatch ILCs. These results indicate that in addition to ILC2s, Arg1 marks a subset of intestinal LTi-like cells in adult cryptopatches.

Arginase-1 expression marks LTi cells and RORγt innate lymphoid populations in the fetal gut

It has been proposed that LTi-like cells in the adult intestinal cryptopatch are analogous to fetal LTi cells at the developing PP, since both of these cell types are RORγt-dependent and they both cluster at VCAM-1⁺ intestinal sites that support B cell accumulation (Eberl, 2005; Eberl & Littman, 2004; Eberl et al, 2004; Kanamori et al, 1996). We therefore set out to determine whether Arg1 is expressed in the fetal intestine during PP organogenesis. In the mouse embryo, LTi cells first begin forming PP anlagen between E15.5-E16.5 in the proximal small intestine (Adachi et al, 1997). At E15.5, hematopoietic YFP⁺ cells were present in the intestine and expressed α4β7, IL-7Rα, c-kit, and low levels of CD11b, but did not express CD11c, CD3, CD19, or

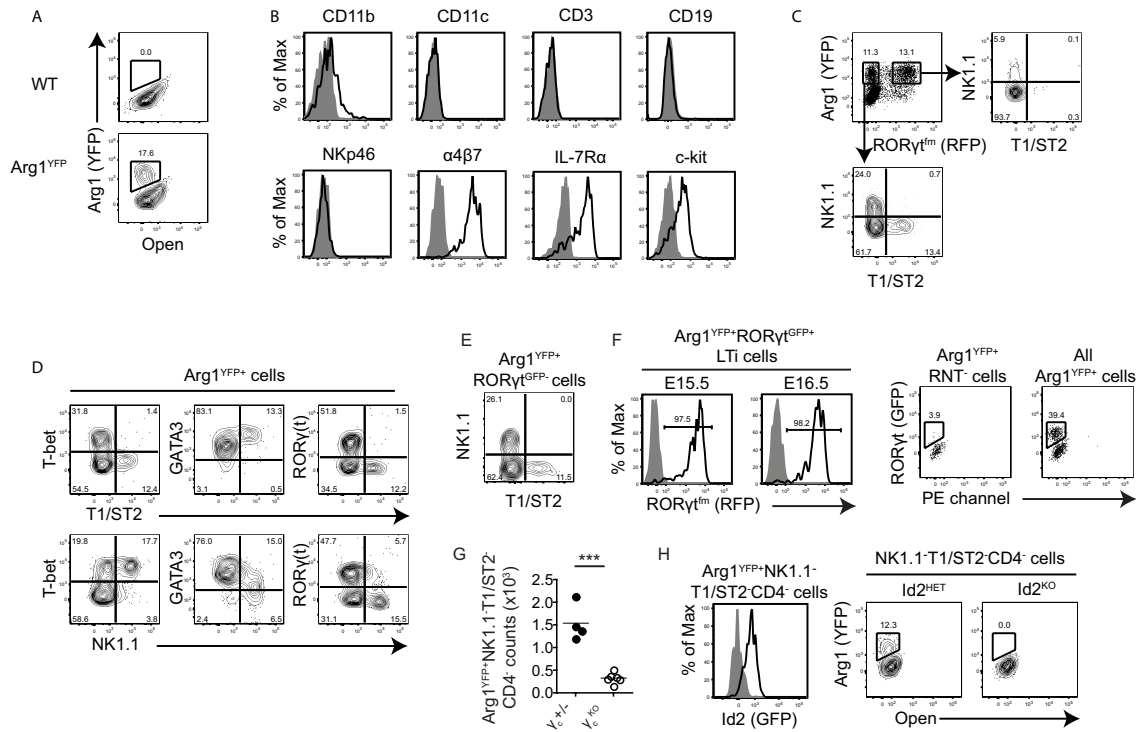


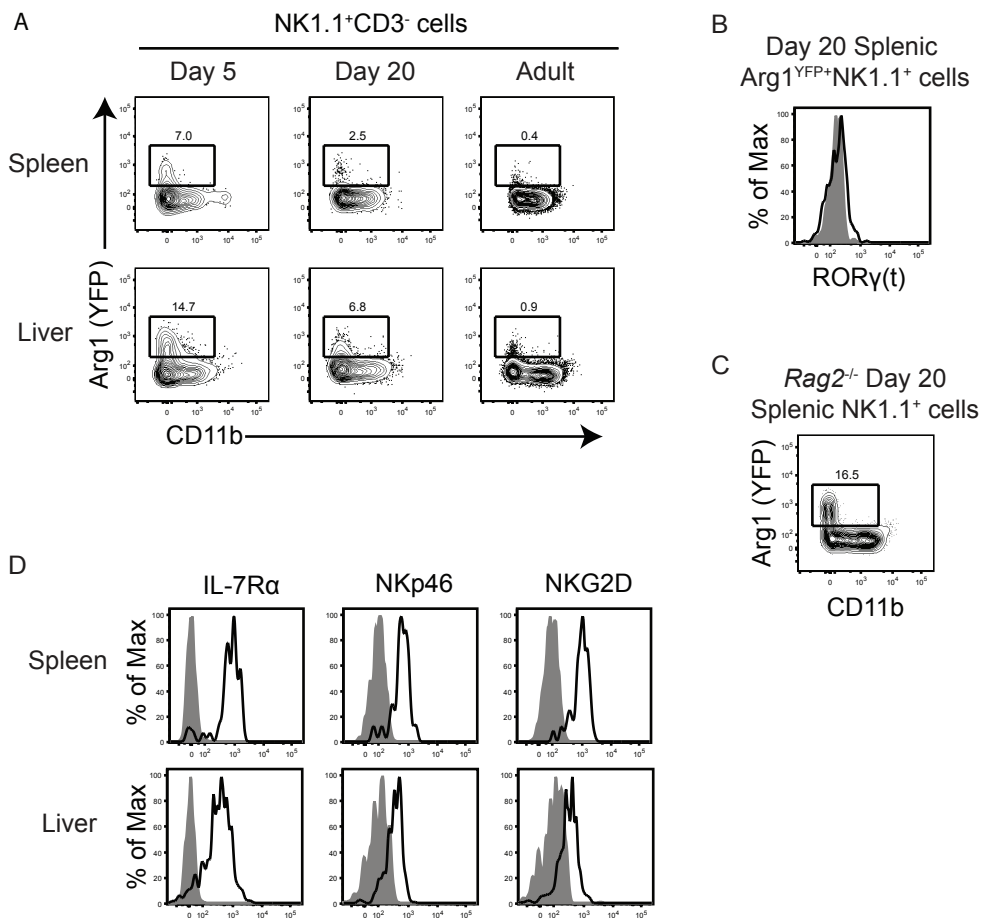
Figure 2. *Arg1* expression marks innate lymphoid populations in the fetal mouse gut.

(A) YFP expression in the E15.5 WT and $Arg1^{YFP}$ intestine. (B) Surface markers expressed by YFP⁺ cells in the E15.5 intestine. (C) RORγ^{fm}, NK1.1, and T1/ST2 expression in distinct $Arg1^{YFP+}$ populations in the E15.5 intestine. $Arg1^{YFP+}RORγ^{fm-}NK1.1^+T1/ST2^-$ ($Arg1^{YFP+}RNT^-$) cells are also present. (D) Expression of T-bet, GATA3, and RORγ(t) in $Arg1^{YFP+}T1/ST2^+$ and $Arg1^{YFP+}NK1.1^+$ cells. (E) $Arg1^{YFP+}RORγ^{GFP-}$ populations in E15.5 intestines from $Arg1^{YFP}/RORγ^{GFP}$ double reporter mice. (F) Comparison of RORγ^{fm} and RORγ^{GFP} reporter mice. Left plots show RFP expression in intestinal $Arg1^{YFP+}RORγ^{GFP+}$ LTi cells from E15.5 and E16.5 $Arg1^{YFP}/RORγ^{fm}/RORγ^{GFP}$ triple reporter mice. Right plots show GFP expression in $Arg1^{YFP+}RNT^-$ cells isolated from E15.5 $Arg1^{YFP}/RORγ^{fm}/RORγ^{GFP}$ intestines (left), or GFP expression in all $Arg1^{YFP+}$ cells from $Arg1^{YFP}/RORγ^{GFP}$ double reporter mice (right) (G) $Arg1^{YFP+}NK1.1^+T1/ST2^-CD4^-$ counts in E15.5 γ_c^{KO} and $\gamma_c^{+/-}$ intestines (n=4-6, representative of 2 independent experiments). *p<0.0001 (H) $Arg1^{YFP+}RNT^-$ cells are dependent on Id2. The left plot shows Id2 (GFP) expression in $Arg1^{YFP+}NK1.1^+T1/ST2^-CD4^-$ cells from E15.5 $Arg1^{YFP}/Id2^{GFP}$ double reporter intestines. Right plots show that $Arg1^{YFP+}NK1.1^+T1/ST2^-CD4^-$ cells are present in $Id2^{+/-}$ intestines and absent in $Id2^{-/-}$ intestines. Plots were previously gated in $CD45^+NK1.1^+T1/ST2^-CD4^-$ cells.

NKp46 (Fig. 2A, B). To determine whether these were LT γ cells, Arg1^{YFP} reporter mice were crossed to ROR γ t-cre/Rosa26-floxSTOP-RFP fate-mapping (ROR γ t^{fm}) mice. Intestinal flow cytometry confirmed that ROR γ t^{fm+} LT γ cells expressed Arg1 (Fig. 2C). Smaller subsets of ROR γ t^{fm+} cells were Arg1^{YFP+}NK1.1⁺ and Arg1^{YFP-}CD11b⁺ (Fig. 2C and data not shown). Our results indicate that ROR γ t⁺ LT γ cells express Arg1 in both the fetal and adult intestine.

In addition to marking ROR γ t^{fm+} LT γ cells, Arg1^{YFP} also marked ROR γ t^{fm-} innate lymphoid cells in the fetal intestine (Fig. 2C). These ROR γ t^{fm-} cells were grouped into three populations based on surface marker and transcription factor expression: NK1.1⁺T-bet⁺ cells, T1/ST2⁺GATA3^{high} ILC2 cells, and a population that lacked NK1.1 and T1/ST2 expression, which we abbreviate here as Arg1^{YFP+}RNT⁻ (Arg1^{YFP+}ROR γ t^{fm-}NK1.1⁻T1/ST2⁻) cells (Fig. 2C, D). The detection of Arg1^{YFP} in fetal ILC2 validated our previous finding that Arg1 expression is a constitutive feature of this cell type (Bando et al, 2013). Arg1^{YFP+}NK1.1⁺ cells were present in the liver and spleen after birth, although the percent of NK1.1⁺ cells that expressed YFP decreased with age (Supplementary Fig. 1A). These cells lacked ROR γ (t) protein expression and were present in 20-day-old *Rag2*^{-/-} mice, indicating that they were neither ILC3s nor iNKT cells (Supplementary Fig. 1B, C). In the adult liver and spleen, Arg1^{YFP+}NK1.1⁺ cells were IL-7R α ⁺NKp46⁺NKG2D⁺ and did not express CD11b (Supplementary Fig. 1A, D). These data indicate that Arg1^{YFP+}NK1.1⁺ cells are members of recently described IL-7R α ⁺NK1.1⁺ ILC1s (Klose et al, 2014).

To validate the existence of the previously undescribed Arg1^{YFP+}RNT⁻ population, YFP⁺ cells were characterized using the ROR γ t^{GFP} 'knock in' reporter mouse



Supplementary Figure 1. **Characterization of Arg1^{YFP}NK1.1⁺ cells.**

(A) YFP expression in NK1.1⁺CD3⁻ cells from the spleen and liver of Arg1^{YFP} mice at different ages post-birth. (B) RORγ(t) protein expression in YFP⁺NK1.1⁺ cells sorted from spleens of 20-day-old Arg1^{YFP} mice. Gray shaded area indicates CD4⁺ T cells. (C) YFP expression in NK1.1⁺ cells from Arg1^{YFP}/Rag2^{-/-} spleens of 20-day-old mice. (D) Expression of IL-7Rα, NKp46, and NKG2D by Arg1^{YFP}NK1.1⁺ cells from adult spleen and liver. Shaded areas indicate isotype controls.

(Eberl et al, 2004). $\text{Arg1}^{\text{YFP}^+}\text{ROR}\gamma\text{t}^{\text{GFP}^-}\text{NK1.1}^-\text{T1/ST2}^-$ cells were present in the fetal intestine at E15.5, confirming the presence of this population (Fig. 2E). To directly compare the two ROR γt reporters, $\text{Arg1}^{\text{YFP}}/\text{ROR}\gamma\text{t}^{\text{GFP}}/\text{ROR}\gamma\text{t}^{\text{fm}}$ triple reporter mice were generated. In these mice, over 95% of intestinal $\text{Arg1}^{\text{YFP}^+}\text{ROR}\gamma\text{t}^{\text{GFP}^+}$ LTi cells were marked by RFP at E15.5 and E16.5, and less than 5% of $\text{Arg1}^{\text{YFP}^+}\text{RNT}^-$ cells expressed ROR $\gamma\text{t}^{\text{GFP}}$ at E15.5, indicating that the two ROR γt reporters are comparable in discriminating fetal intestine $\text{Arg1}^{\text{YFP}^+}\text{RNT}^-$ cells (Fig. 2F). Similar to other ILC populations, $\text{Arg1}^{\text{YFP}^+}\text{RNT}^-$ cells (estimated by staining for $\text{Arg1}^{\text{YFP}^+}\text{NK1.1}^-\text{T1/ST2}^-\text{CD4}^-$ cells) were dependent on γc and Id2 (Fig. 2G, H). Thus, $\text{Arg1}^{\text{YFP}^+}\text{RNT}^-$ cells are an ILC population in the fetal mouse intestine with unknown lineage specificity. Taken together, our results indicate that $\text{IL-7R}\alpha^+\text{NK1.1}^+$ ILC1s, ILC2s, LTi ILC3s, and an uncategorized RNT^- ILC population express Arg1 in the fetal intestine.

Fetal $\text{Arg1}^{\text{YFP}^+}\text{RNT}^-$ cells aggregate at the Peyer's patch anlage in a lymphotoxin-dependent manner

To determine where $\text{Arg1}^{\text{YFP}^+}\text{RNT}^-$ cells accumulate in the intestine, we examined the location of YFP^+ cells in the developing gut. The most proximal PP begins to develop between E15.5-E16.5, with PPs distal to the first site developing sequentially over the next few days (Adachi et al, 1997). At E14.5-E15, $\text{Arg1}^{\text{YFP}^+}$ LTi and RNT^- cells were most abundant in the upper and middle portions of the small intestine, indicating that these ILCs are locally positioned prior to the development of proximal PP anlagen (Fig. 3A). At E16.5, $\text{Arg1}^{\text{YFP}^+}$ cells were present at the first developing VCAM-1^+ PP anlage (Fig. 3B), and consisted of both $\text{ROR}\gamma\text{t}^{\text{fm}^+}$ LTi cells and $\text{ROR}\gamma\text{t}^{\text{fm}^-}$ cells (Fig. 3C). To quantify $\text{Arg1}^{\text{YFP}^+}\text{ROR}\gamma\text{t}^{\text{fm}^-}$ populations at the anlage, LTi

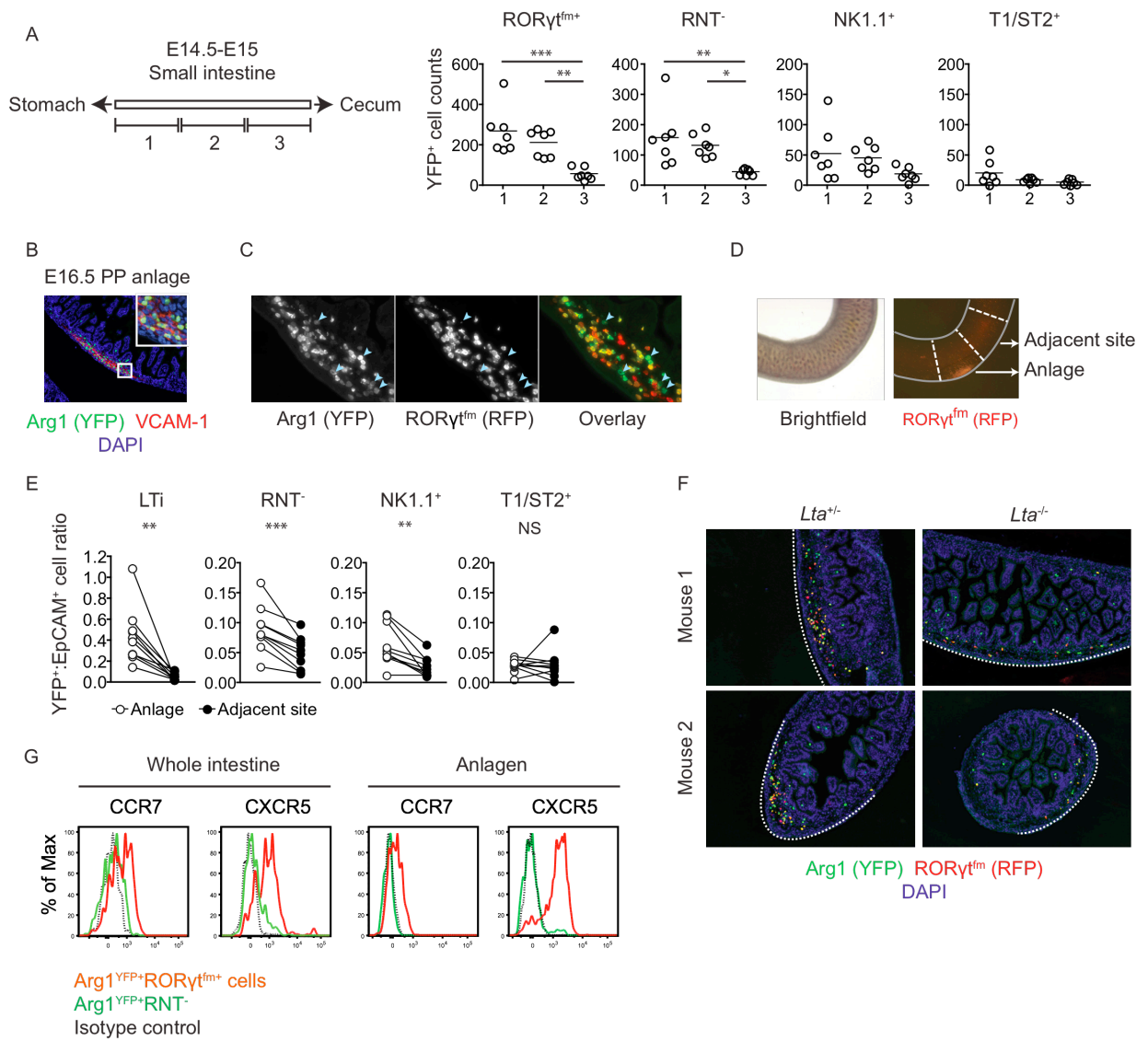
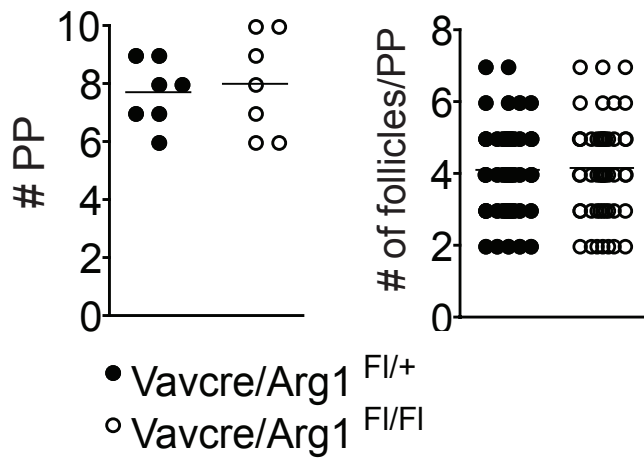


Figure 3. **Fetal Arg1^{YFP+}RNT cells aggregate at the Peyer's patch anlage in a lymphotoxin-dependent manner.** (A) YFP⁺ cell counts from upper, middle, and lower sections of the E14.5-E15 small intestine. *p<0.05, **p≤0.01, ***p≤0.001 (B) YFP⁺ cells at the PP anlage in the E16.5 intestine. The anlage was identified by VCAM-1⁺ stromal cells, and sections were counterstained with DAPI. (C) Arg1 (YFP) and RORγt^{flm} (RFP) expression at the anlage of E16.5 Arg1^{YFP}/RORγt^{flm} double reporter mice. Blue arrowheads point at examples of YFP⁺RFP⁻ cells. (D) Identification of the anlage in intact E16.5 Arg1^{YFP}/RORγt^{RFP} intestines. (E) Ratio of YFP⁺ populations to EpCAM⁺ cells in dissected anlagen and adjacent sites (n=10, pooled from 2 independent experiments). **p≤0.01, ***p≤0.001 (F) Arg1 (YFP) and RORγt^{flm} (RFP) expression in sections of *Lta*^{+/-} (left images) and *Lta*^{-/-} littermates (right images). *Lta*^{+/-} images are of PP anlagen, while *Lta*^{-/-} images are representative of sections through the intestines of 3 litters. Dotted white lines indicate the anti-mesenteric side of each intestine. (G) Expression of CCR7 and CXCR5 in Arg1^{YFP+}RNT⁻ cells and Arg1^{YFP+}RORγt^{flm+} LTi cells from whole intestines (left plots) or dissected anlagen (right plots).

clusters were identified by RFP expression in whole intestines and dissected for flow cytometric analysis (Fig. 3D). At E16.5, the first developing PP contained significantly more Arg1^{YFP+}RNT⁻ and Arg1^{YFP+}NK1.1⁺ cells than sites immediately adjacent to the developing organ based on the ratio of YFP cells to CD45⁻EpCAM⁺ cells (Fig. 3E). In contrast, Arg1^{YFP+}T1/ST2⁺ ILC2s did not accumulate at the anlage.

The PP anlage is formed when stromal cells at the anti-mesenteric side of the intestine are activated at discrete sites by LT α 1 β 2⁺ hematopoietic cells (Honda et al, 2001). To test whether fetal Arg1^{YFP+}RNT⁻ accumulation at the anlage was dependent on stromal activation, E16.5 *Lta*^{-/-} intestines were assessed for YFP⁺ aggregates by sectioning through the intestine. RFP⁺ LTi cells and YFP⁺RFP⁻ cells were enriched at the anti-mesenteric side of the intestine in *Lta*^{-/-} and *Lta*^{+/-} littermates (Fig. 3F). However, aggregated clustering of YFP⁺ cells was dependent on *Lta*. This suggested that factors induced by LT α 1 β 2 actively recruit or tether Arg1^{YFP+}RNT⁻ cells to the PP anlage. LT α 1 β 2 activates expression of the chemokines CXCL13 and CCL19 in intestinal LTo cells in situ, and LTi cells migrate towards these chemokines in vitro (Honda et al, 2001; Okuda et al, 2007). Compared to LTi cells, which express the chemokine receptors CXCR5 and CCR7, Arg1^{YFP+}RNT⁻ cells did not express these receptors even after restricting our analysis to cells from the anlage (Fig. 3G). We conclude that Arg1^{YFP+}RNT⁻ cells accumulate at the PP anlage in a CCR7- and CXCR5-independent manner after LT β R signaling is activated in stromal LTo cells.

Although multiple ILC populations express Arg1 at the developing PP, Arg1 expression by hematopoietic cells was not required for normal numbers of PP or PP follicles as assessed in *Vav-cre/Arg1*^{fl/fl} adult mice (Fig. S2). Mice deficient in



Supplementary Figure 2. **Arg1 is not required for PP development.**

PP numbers per intestine (left) and follicles per PP (right) in Vav-cre/Arg1^{flox/flox} mice and Vav-cre/Arg1^{flox/+} controls.

hematopoietic Arg1 also had normal B and T cell compartmentalization in the PP, inguinal lymph node, and spleen (data not shown).

Arg1^{YFP+}RNT⁻ cells are fetal ILC precursors

Before PP development, at E13.5, Arg1^{YFP+}RNT⁻ cells were the most abundant YFP⁺ ILC lineage in the fetal intestine (Fig. 4A). As the frequency of YFP⁺ cells that were RORγt^{fm+} LTi cells increased over 3 days, the percent of RNT⁻ cells decreased. These data suggest that Arg1^{YFP+}RNT⁻ cells in the fetal intestine are ILC precursors that undergo differentiation into other ILC lineages. In adult BM, ILC precursors express GATA3 but lack T-bet and RORγt (Klose et al, 2014). In contrast, Arg1^{YFP+}RNT⁻ cells in the E15.5 intestine expressed all three transcription factors, as assessed by intracellular staining (Fig. 4B). Arg1^{YFP+}RNT⁻ cells that expressed RORγ(t) protein could be distinguished from RORγt^{fm+} cells by their higher levels of GATA3 and T-bet (Fig. 4C). Additionally, fetal Arg1^{YFP+}RNT⁻ cells expressed higher levels of CD45 than RORγt^{fm+} LTi cells and did not express the surface trimer LTα₁β₂ (Fig. 4D). Similarly, Arg1^{YFP+}RNT⁻ cells that expressed T-bet expressed more GATA3 and RORγ(t) protein than mature Arg1^{YFP+}NK1.1⁺ cells (Fig. 4E). Therefore, Arg1^{YFP+}RNT⁻ cells in the fetal intestine express multiple transcription factors associated with mature ILC populations, but lack the distinct protein expression profiles associated with any one specific ILC lineage. Collectively, these data suggest that intestinal Arg1^{YFP+}RNT⁻ cells are ILC precursors that are in a transitional state as they develop into mature ILC populations.

To test whether Arg1^{YFP+}RNT⁻ cells were ILC precursors, cells were isolated from E15.5 intestines by flow cytometric cell sorting and cultured in vitro with recombinant mouse IL-7 (Fig. 5A). By 20 h, Arg1^{YFP+}RNT⁻ cells gave rise to RORγt^{fm+}, RORγt^{fm-}

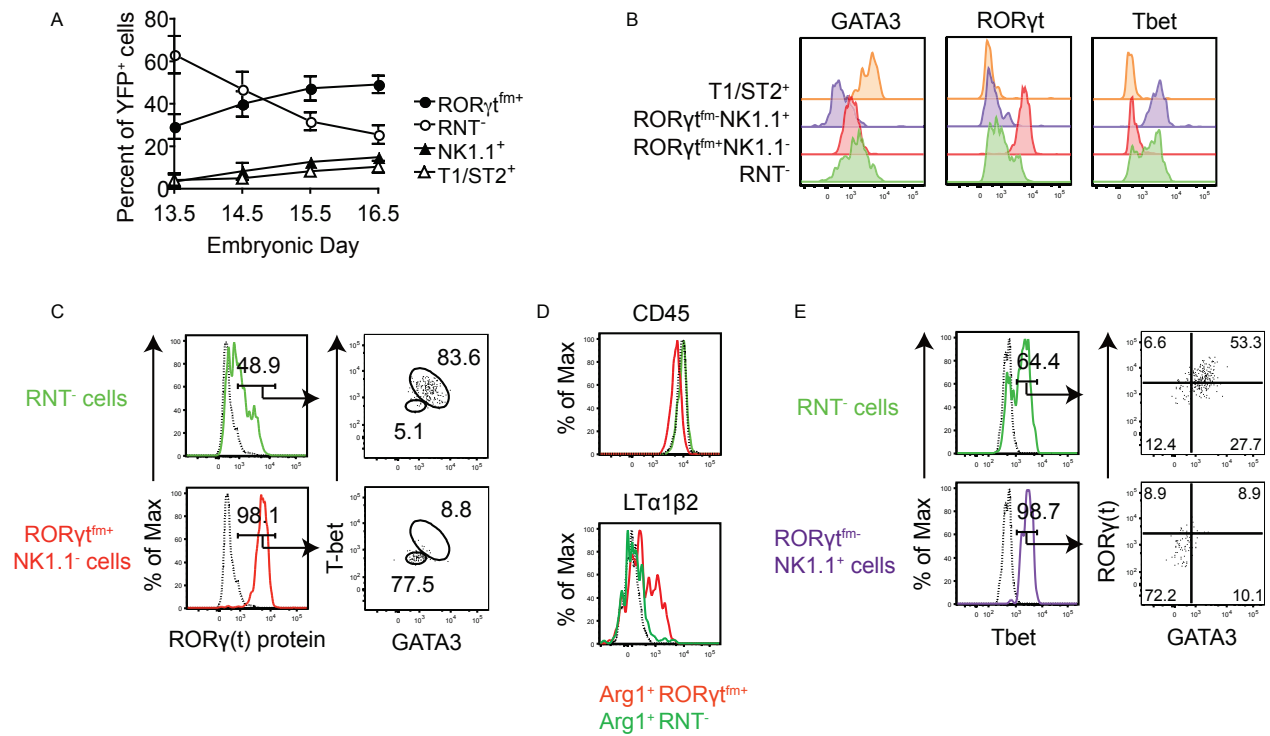


Figure 4. **Characterization of Arg1^{YFP+} RNT⁻ cells.**

(A) The frequency of each ILC population as a percent of total YFP⁺ cells (n=5-7, pooled from 2 independent experiments). (B) Transcription factor expression in Arg1^{YFP+} RNT⁻ cells compared to other Arg1^{YFP+} ILC populations. (C) GATA3 and Tbet expression in RORγ(t) protein-expressing RNT⁻ cells compared to RORγ^{fm}⁺ cells. (D) CD45 and LTα₁β₂ expression in Arg1^{YFP+} RNT⁻ cells and Arg1^{YFP+} RORγ^{fm}⁺ LTi cells. The dotted black line represents ILC2s in the CD45 plot, and Ig control in the LTα₁β₂ plot. (E) RORγ(t) and GATA3 protein expression in Tbet-expressing RNT⁻ cells compared to RORγ^{fm}⁻ NK1.1⁺ cells.

NK1.1⁺, and T1/ST2⁺ cells (Fig. 5B). RORyt^{fm+} cells that developed in culture did not express CD3 or NKp46 at day 6 (Fig. 5C). Because a small percentage of Arg1^{YFP+}RNT⁻ cells expressed CD25 (Fig. 5D), we excluded these cells by sorting and culturing Arg1^{YFP+}RNT⁻CD25⁻ cells in subsequent experiments. An analysis of transcription factors after 6 days of culture with OP9 cells indicated that Arg1^{YFP+}RNT⁻CD25⁻ cells gave rise to NK1.1⁺RORyt^{fm-}T-bet⁺GATA3⁻ ILC1s, RORyt^{fm-}NK1.1⁻CD25⁺ICOS^{hi}GATA3⁺T-bet⁻ ILC2s, and RORyt^{fm+}T-bet⁻GATA3⁻ ILC3s (Fig. 5E, F). No CD5, CD19, or CD11b⁺ cells were present in cultures at day 6 (Fig. 5G). Although YFP and T1/ST2 were present after 20 hours, these proteins were not detected at day 6 of culture, indicating that additional factors are required to maintain expression of Arg1 and IL-33R in fetal cells (data not shown).

To test further whether fetal Arg1^{YFP+}RNT⁻CD25⁻ cells were precursors to Arg1^{YFP+} ILC lineages, we cultured single cells with OP9 cells. At 6 days, the majority of wells contained homogeneous populations of RORyt^{fm-}NK1.1⁺ (35.7%), RORyt^{fm-}NK1.1⁻CD25⁺ICOS⁺ (16.6%), or RORyt^{fm+}NK1.1⁻ cells (23.6%), indicating that Arg1^{YFP+}RNT⁻CD25⁻ cells can become ILC1s, ILC2s, and ILC3s (Fig. 5H, I). Cells that were NK1.1⁺RORyt^{fm+} and express T-bet were present in <2% of wells, and represent a population of NK1.1⁺ cells that temporally expresses RORyt during development (Fig. 5I and data not shown) (Klose et al, 2012; Vonarbourg et al, 2010). Five percent of wells contained an undetermined population that did not express the lineage markers used in these experiments. Wells that contained 2 populations (18.5%) consisted primarily of the undetermined population with RORyt^{fm+}NK1.1⁻ cells (23.3%) or RORyt^{fm-}NK1.1⁺

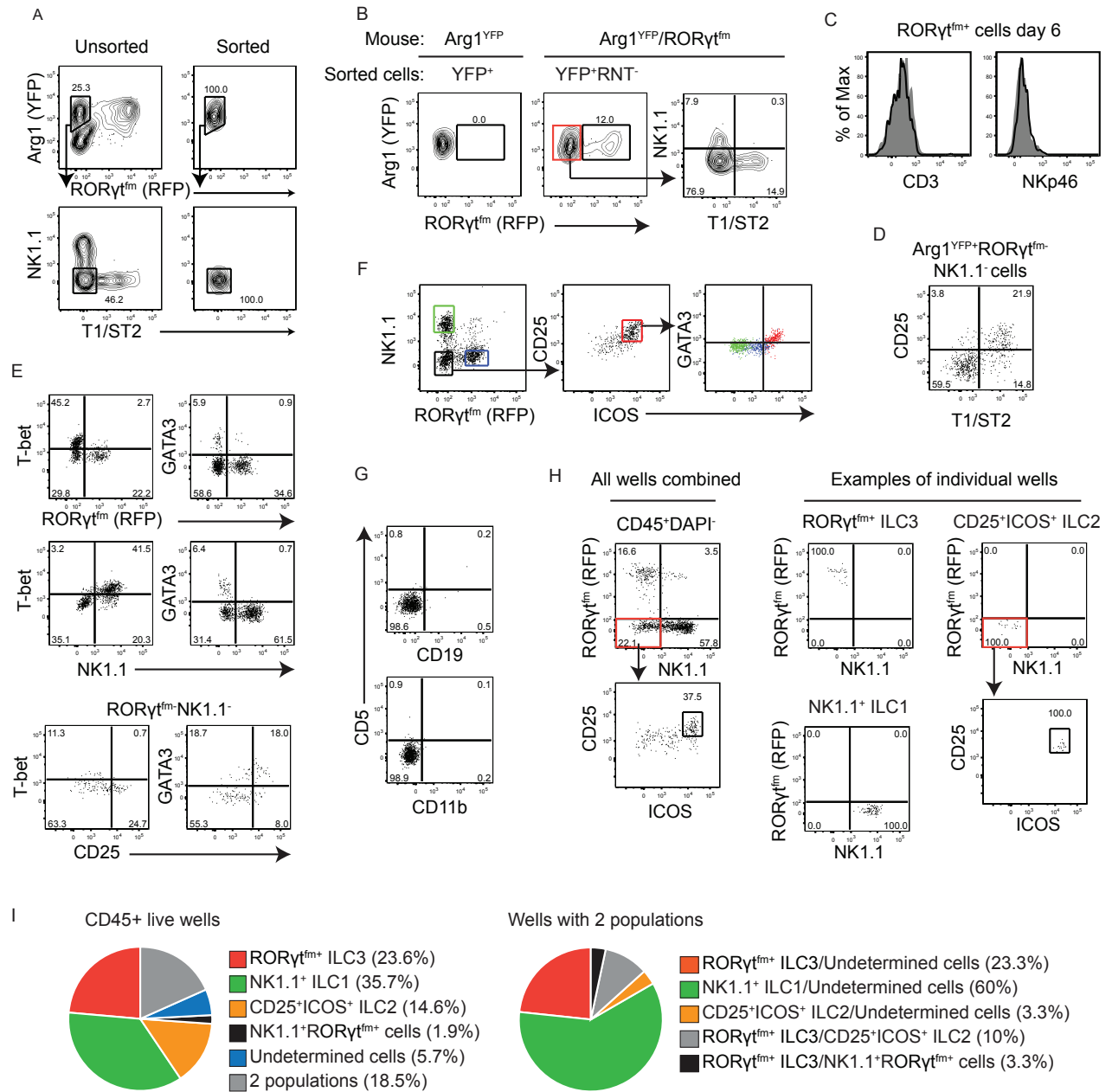


Figure 5. ***Arg1^{YFP+}RNT⁻ cells are fetal ILC precursors.***

(A) Purity of sorted Arg1^{YFP+}RNT⁻ cells (right plots) compared to unsorted cells (left plots). (B) Populations detected after culturing Arg1^{YFP+}RNT⁻ cells for 20 hr. The left plot represents cultured Arg1^{YFP} single reporter cells, while right plots are from Arg1^{YFP}/RORγt^{fm} double reporter mice. (C) Expression of CD3 and NKp46 in RORγt^{fm+} cells after 6 days. (D) CD25 expression in Arg1^{YFP+}RORγt^{fm-}NK1.1⁻ cells. (E) Transcription factors expressed by RORγt^{fm+}, NK1.1⁺, and RORγt^{fm-}NK1.1⁻CD25⁺ cells after 6 days of culturing Arg1^{YFP+}RNT⁻CD25⁻ cells with OP9 cells. (F) ICOS expression in NK1.1⁻RORγt^{fm-}CD25⁺ cells (red) compared to NK1.1⁺ (green) and RORγt^{fm+} (blue) populations at day 6 of culture. (G) CD5, CD19, and CD11b expression at day 6 of culture. (H) Examples of gates used to identify populations in single cell cultures at day 6. Left plots are combined files of single wells from a 96 well plate. Right plots are examples of individual wells from single cell cultures at day 6. The top left, bottom left, and right plots show different ILC populations from 3 separate wells. (I) Cell populations isolated from wells from single cell cultures at day 6 (left) and breakdown of wells that contained 2 populations (right). Undetermined cells did not express markers used to identify other lineages. Data are pooled from 3 independent experiments.

ILC1s (60%). These data indicate that $\text{Arg1}^{\text{YFP}^+}\text{RNT}^-$ cells in the intestine are extrahepatic fILCPs that give rise to Arg1^+ ILC lineages found in vivo.

The fetal liver and adult BM contain $\text{Lin}^- \text{Id2}^+ \text{IL-7R}\alpha^+ \alpha 4\beta 7^+ \text{flt3}^- \text{CD25}^-$ ILC precursors, which are distinguished from CLP by flt3 and from ILC2 precursors by CD25 (Klose et al, 2014). In the Arg1^{YFP} E14.5-E15 fetal liver, $\text{Lin}^- \text{IL-7R}\alpha^+ \alpha 4\beta 7^+ \text{CD25}^- \text{T1/ST2}^-$ cells were flt3^- and >70% of these cells expressed YFP (Fig. 6A). In $\text{Arg1}^{\text{YFP}}/\text{Id2}^{\text{GFP}}$ double-reporter mice, 80% of $\text{Lin}^- \text{Id2}^{\text{GFP}^+} \text{IL-7R}\alpha^+ \alpha 4\beta 7^+ \text{CD25}^- \text{T1/ST2}^-$ fetal liver ILC precursors expressed YFP, confirming that $\text{Arg1}^{\text{YFP}^+}\text{RNT}^-$ cells are fILCP as determined by previously reported markers (Fig. 6B). In contrast, $\text{Arg1}^{\text{YFP}^+}$ cells in adult BM consisted of only CD25^+ and/or T1/ST2^+ ILC2 cells (Fig. 6C) (Hoyler et al, 2012). Arg1^{YFP} and $\text{Arg1}^{\text{YFP}}/\text{Id2}^{\text{GFP}}$ mice confirmed that $\text{Lin}^- \text{IL-7R}\alpha^+ \alpha 4\beta 7^+$ cells in adult BM did not express flt3 , and $\text{Lin}^- \text{Id2}^{\text{GFP}^+} \text{IL-7R}\alpha^+ \alpha 4\beta 7^+ \text{CD25}^-$ precursors did not express Arg1 (Fig. 6C, D). These data show that based on previously reported methods for identifying ILC precursors, Arg1 is expressed by ILC precursors in the fetus and not the adult, indicating differences in gene expression by this cell type during these two stages of life.

Discussion

ILCs have critical functions in organogenesis, homeostasis, and immunity, but their development in the fetal mouse is not fully characterized. Here, we show that Id2 -dependent Arg1^+ fILCP are present in the fetal intestine, and have the capacity to develop into ILC1s, ILC2s, and ILC3s. $\text{Arg1}^+\text{RNT}^-$ cells expressed GATA3, T-bet, and ROR γ t in combinations that were distinct from mature ILC lineages, and did not express

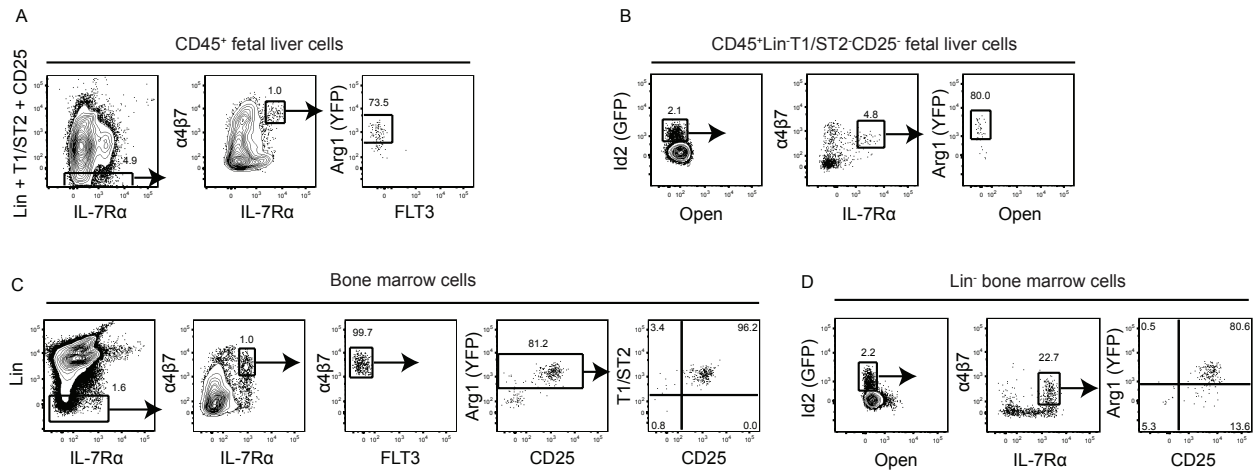


Figure 6. *Arg1*^{YFP} expression by ILC precursors in fetal liver and adult bone marrow.

(A) YFP expression in E14.5-E15 CD45⁺Lin⁻T1/ST2⁻CD25⁻IL-7Rα⁺α4β7⁺flt3⁻ cells from *Arg1*^{YFP} reporter mice. (B) *Arg1* expression in CD45⁺Lin⁻T1/ST2⁻CD25⁻Id2^{GFP}IL-7Rα⁺α4β7⁺ ILC precursors from *Arg1*^{YFP}/Id2^{GFP} double reporter mice. (C) Expression of CD25 and T1/ST2 in Lin⁻IL-7Rα⁺α4β7⁺flt3⁻YFP⁺ cells from *Arg1*^{YFP} adult bone marrow. (D) YFP expression in Lin⁻Id2^{GFP}IL-7Rα⁺α4β7⁺ cells from *Arg1*^{YFP}/Id2^{GFP} adult bone marrow.

surface markers of mature ILCs. In contrast, Id2⁺ multipotent ILC progenitors described in adult bone marrow do not express ROR γ t or T-bet (Klose et al, 2014). These data suggest that Arg1⁺ fILCP in the intestine may occupy an intermediate developmental step between undeveloped GATA3⁺T-bet⁻ROR γ t⁻ ILC precursors and fully differentiated ILC populations. These data support a model in which ILC precursors leave the fetal liver and enter other organs, where they go through a transitional developmental stage before completing their differentiation into mature ILC lineages. Previous work has shown that GATA3⁺T-bet⁻ROR γ t⁻ ILC precursors are absent in the adult intestine (Klose et al, 2014). Further studies will be necessary to determine whether GATA3⁺T-bet⁺ROR γ t⁺ ILC precursors are present in the adult gut or whether ILC precursor dispersal into tissue only occurs during early life. Specific immune populations, such as microglia and Langerhans cells, have been shown to have fetal origins under homeostatic conditions, but whether this is the case for tissue ILC populations is unknown (Ginhoux et al; Hoeffel et al, 2012).

The difference in Arg1 expression in fetal and adult BM ILC precursors indicates that there is differential gene regulation in this population at these two life stages. However, since these data are based on reported markers for ILC precursors, additional work is required to confirm that Arg1⁺ cells in the fetal liver are multipotent precursors. Future studies may focus on identifying whether there are additional genes that distinguish ILC precursors in the fetus and adult, and whether Arg1⁺ fetal ILC precursors differ in function from adult cells. While Arg1 expression in myeloid cells is induced by STAT6 or MyD88 activation, Arg1 expression in ILC populations occurs under homeostatic conditions (Bando et al, 2013; El Kasmi et al, 2008; Herbert et al, 2004;

Hesse et al, 2001; Munder et al, 1998). Recently, Arg1 was identified as one of many genes that is dependent on GATA3 in ILC2s and ILC3s in vitro (Yagi et al, 2014). However, GATA3⁺ type 2 CD4⁺ T cells in the helminth-infected lung and GATA3⁺ precursors in adult BM do not express Arg1, indicating that this transcription factor is not sufficient for enzyme expression in lymphoid cells (Bando et al, 2013). Further studies will be required to identify additional factors that regulate Arg1 in different ILC populations.

In contrast to ILC precursors in the fetal liver, Arg1⁺ ILC precursors in the fetal intestine are a uniquely localized source of LTi cells at sites that require their rapid accumulation. Here, we show that ILC precursors preferentially accumulate at the developing PP at E16.5 as compared to adjacent areas. Recently, CD45⁺IL-7R α ⁺SCA-1⁺CD4⁻ cells have been found at the lymph node anlage as early as E13.5 (van de Pavert et al, 2014). Whether this population contains precursors that give rise to multiple ILC lineages during lymph node development remains unknown. In the intestine, we determined that Arg1⁺RNT⁻ accumulation at the PP was dependent on LT α , indicating that this event occurs after LTi cells initiate organogenesis. LT α ₁ β ₂ induces the expression of adhesion molecules and chemokines at the PP anlage, and identifying which factors are required for accumulation will be critical to test the effects of cell localization. Intestinal Arg1⁺ ILC precursors are unable to initiate the development of lymphoid organs because they lack LT α ₁ β ₂ expression, but may enhance the positive feedback loop once at the PP anlage by providing additional ILC3s on site. By this model, stochastically differentiated LTi cells that induce PP development at E15.5-E16.5 initiate a LT β R-signaling program in LTo cells necessary for the aggregation of fILCPs

at the PP, thus providing a localized source of ILC populations resident in the fetal gut. We suggest that this system reinforces stromal cell activation at each PP while maintaining normal numbers of lymphoid organs.

Methods

Mice

Arg1^{YFP} (YARG) mice have been previously described (Reese et al, 2007). RORyt^{GFP}, Id2^{GFP}, CD132^{-/-}, Arg1^{flox}, and wildtype C57BL/6 mice were purchased from the Jackson Laboratory (Bar Harbor, ME). *Rag2*^{-/-} mice were purchased from Taconic (Hudson, NY). Drs. Dean Sheppard (University of California, San Francisco) and Dimitris Kioussis (MRC National Institute for Medical Research, London) kindly provided Vav-cre mice (de Boer et al, 2003). RORyt-cre Tg mice were provided by Dr. Dan Littman (New York University) (Eberl & Littman, 2004). Rosa26-flox-STOP-RFP mice were provided by Drs. Ellen Robey (University of California, Berkeley), Herve Luche, and Hans Jorg Fehling (University Clinics Ulm) (Luche et al, 2007). In Arg1^{YFP}/RORyt-cre/Rosa26-flox-STOP-RFP crosses, Arg1^{YFP} and Rosa26-flox-STOP-RFP were kept homozygous in both male and female breeders. We found that using male breeders that carried both RORyt-cre and Rosa26-flox-STOP-RFP alleles led to sporadic germline transmission of RFP in progeny. Thus, in all experiments RORyt-cre was carried only by female breeders to prevent germline RFP expression. Fetal mice were genotyped by tail PCR and flow cytometry of spleens. In experiments with Vav-cre, cre was also only carried by female breeders. All mice were backcrossed to the C57BL/6 background for at least 7 generations. All experiments were conducted according to protocols approved by the UCSF Institutional Animal Care and Use Committee.

Tissue dissociation

Small intestines from adult mice were flushed with PBS and PP were removed. Intestines were filleted, rinsed, chopped into 5 mm pieces and digested with collagenase VIII (Sigma, St. Louis, MO) and DNase I (Roche Diagnostics, Indianapolis, IN) at 37°C for four rounds of 35-minute incubations. Final digested samples were then centrifuged on a 40%/90% Percoll gradient (GE Healthcare Biosciences, Pittsburgh, PA).

Detection of c-kit and CD4 was reduced by the intestinal cell isolation protocol, and were thus assayed on cells obtained by directly dissecting cryptopatches. Briefly, intestines were filleted and laid flat on glass slides. Cryptopatches were identified under a microscope and biopsied out of the tissue with the use of a flexible plastic needle. Biopsies were gently crushed through a 70-micron filter to obtain a single cell suspension.

To obtain cells from the fetal mouse gut, intestines were first isolated from embryos under a dissecting microscope, and then further dissected under magnification to remove the associated mesenteric tissue. In experiments where the intestine was segmented into upper, middle, and lower regions, the small intestine was divided into three equal portions using a ruler. Intestines were digested with dispase (Gibco, Grand Island, NY) and DNase I (Roche Diagnostics) at 37°C for 25 minutes and mechanically dissociated using a gentleMACS Dissociator (Miltenyi Biotec, San Diego, CA). Tissue homogenates were then passed through a 70-micron filter.

PP anlagen were dissected from embryonic intestines under a fluorescent dissecting microscope. ROR γ ^{flm+} cell aggregates were used as markers for developing PPs. Anlagen were digested, mechanically dissociated, and filtered as described above.

Flow cytometry

Rat anti-mouse CD4 (RM4-5), rat anti-mouse CD11b (M1/70), Armenian hamster anti-mouse CD11c (HL3), rat anti-mouse CD19 (ID3), rat anti-mouse CD25 (7D4), rat anti-mouse B220 (RB6-8C5), and rat anti-mouse CXCR5 (2G8) antibodies were purchased from BD Pharmingen (San Diego, CA); rat anti-mouse c-kit (2B8), rat anti-mouse CD3 (17A2), rat anti-mouse CD5 (53-7.3), rat anti-mouse CD25 (eBio7D4), rat anti-mouse CD127 (A7R34), rat anti-mouse NKp46 (29A1.4), rat anti-mouse LPAM (DATK32), rat anti-mouse CCR7 (4B12), rat anti-human/mouse GATA3 (TWAJ), rat anti-mouse ROR γ (t), and mouse anti-mouse NK1.1 (PK136) antibodies were purchased from eBioscience (San Diego, CA); rat anti-mouse CD45 (30-F11), rat anti-mouse Ter119 (TER-119), mouse anti-human/mouse T-bet (2B10), Armenian hamster anti-human/mouse/rat ICOS (C398.4A), rat anti-mouse CD25 (PC61), and rat anti-mouse flt3 (A2F10) antibodies were purchased from Biolegend (San Diego, CA); and rat anti-mouse T1/ST2 (DJ8) antibodies were purchased from MD Bioproducts (St Paul, MN). LTBR-Ig fusion protein and Ig control was purchased from R&D Systems (Minneapolis, MN). PE-cy7-conjugated streptavidin was purchased from BD Biosciences (San Jose, CA) and APC-conjugated streptavidin was purchased from eBioscience. Live/dead (Invitrogen, Grand Island, NY) or DAPI was used to exclude dead cells. Cells were sorted with an Aria II or MoFlo prior to intracellular staining due to loss of YFP during fixation. In experiments where transcription factors were assessed in Arg1^{YFP+}RNT⁻

cells, Arg1^{YFP+}RFP⁻ cells (consisting of RNT⁻, NK1.1⁺ and T1/ST2⁺ cells) were sorted to 99% purity into a single tube prior to intracellular staining. Arg1^{YFP+}RORγt^{fm+} cells were sorted in parallel. In fetal liver experiments, Lin⁻ cells were defined as lacking CD3, CD4, CD5, CD19, NK1.1, Ter119, Gr-1, and CD11b. In adult BM experiments, Lin⁻ cells were defined as lacking CD3, CD4, CD5, CD19, NK1.1, Ter119, Gr-1, and B220.

Transcription factors were analyzed using the Foxp3/Transcription Factor Staining Buffer Set from eBioscience. In experiments where RFP detection was required after intracellular staining, cells were fixed in 2% paraformaldehyde (PFA) for 2 minutes and washed with PBS prior to fixation with reagents from the Transcription Factor Staining Buffer set. For LTα₁β₂ detection, cells were blocked with donkey anti-mouse Fab fragments (Jackson ImmunoResearch, West Grove, PA) prior to staining with LTβR-Ig. Cells were stained with biotin-conjugated donkey anti-mouse IgG (Jackson ImmunoResearch) and blocked with mouse serum before incubating cells with antibodies and APC-conjugated streptavidin. Counting beads were used to determine total cell numbers (CountBright absolute counting beads, Invitrogen). Flow cytometry was performed using a LSR II (BD Biosciences).

Immunohistochemistry

Samples were fixed with 4% PFA (Electron Microscopy Sciences, Hatfield, PA) in PBS for 2 hours, and then left in PBS overnight. Tissues were then incubated in 30% sucrose for 2 hours before they were frozen in OCT compound (Sakura, Torrance, CA). Frozen tissue blocks were sectioned at 8 microns (adult gut) or 7 microns (fetal gut) using a Leica CM3050-S cryostat. In experiments with *Lta*^{-/-} animals, serial sections

were taken of the proximal half of the small intestine (where the first PP develops), and every section was analyzed for YFP⁺ aggregates.

Sections were incubated with 3% H₂O₂/0.1% NaN₃ in PBS for 45 minutes to quench endogenous peroxidase, and then blocked with rat anti-mouse CD16/CD32, 1% mouse serum, and 1% rat serum for 1 hour. Endogenous biotin and avidin-binding sites were blocked with a Biotin/Avidin Blocking Kit (Vector Labs, Burlingame, CA). Slides were incubated with biotin-conjugated goat anti-GFP (Abcam, San Francisco, CA), biotin-conjugated rabbit anti-RFP (Abcam), or biotin-conjugated rat anti-mouse VCAM-1 biotin (eBioscience) for 1-2 hr followed by HRP-conjugated streptavidin (Perkin Elmer, Waltham, MA) and FITC- (Perkin Elmer) or A555-conjugated tyramide (Invitrogen). Sections that were stained with two biotinylated antibodies were treated with H₂O₂/NaN₃ and avidin/biotin blocking reagents prior to each antibody incubation. In other experiments, sections were stained with rat anti-mouse RORγ(t) (B2D, eBioscience). DAPI was added to sections for 5 minutes to visualize nuclei.

Cell culture

Cells were sorted on an Aria II (BD Biosciences) and cultured with 10 ng/ml recombinant mouse IL-7 (R&D Systems) in RPMI 1640 medium (supplemented with HEPES, fetal calf serum (10%), sodium pyruvate, 2-mercaptoethanol, streptomycin/penicillin, and L-glutamine) for 20 hr or 6 days at 2-5 x 10³ cells/well. In other experiments, 1.5 x 10³ cells or single cells were sorted into 96-well plates containing 1.2 x 10⁴ irradiated OP9 cells/well (American Type Culture Collection, Manassas, VA), 10 ng/ml recombinant IL-7, and 10 ng/ml rSCF (R&D Systems). Media

was replenished on the third day and wells were analyzed by flow cytometry on day 6. At the time of analysis (day 6), $50.4 \pm 5.5\%$ of wells contained live CD45⁺ cells.

Statistics

Data were analyzed with Prism (GraphPad Software, La Jolla, CA) using the two-tailed unpaired or paired Student's *t*-test, or one-way ANOVA followed by Tukey's test.

Acknowledgements

The authors thank V. Nguyen from the UCSF Flow Cytometry Core and Z. Wang from the Sabre Sorting Facility for cell sorting. We thank Drs. D. Sheppard, D. Kioussis, D. Littman, E. Robey, H. Luche and H. J. Fehling for mice. We thank Drs. J. Cyster and L. Lanier for critical reading of the manuscript. Supported by Howard Hughes Medical Institute; grants AI026918, AI030663, and AI119944 from the NIH; and the Sandler Asthma Basic Research Center at UCSF. JKB received support from the Biomedical Sciences (BMS) Graduate Program.

Chapter Four:

Discussion

A revised section of the text in this chapter has been submitted as: Bando JK, Liang H-E, Locksley RM. Identification and distribution of ILC precursors in the fetal mouse intestine.

ILC precursors with an intermediate differentiation phenotype

In the past few years, new subsets of ILCs have been characterized that contribute to the maintenance of homeostasis and the host response to pathogens. How these cells develop throughout the life of the animal is a topic under active investigation. Recent reports have demonstrated that multipotent ILC precursors in the fetal liver and adult bone marrow give rise to ILC1, ILC2, and ILC3 populations (Constantinides et al, 2014; Klose et al, 2014). Here, I show that fetal cells that differentiate into mature ILC populations *in vitro* are also marked by the urea cycle enzyme Arg1. These cells are termed “Arg1⁺RNT⁻” due to their lack of ROR γ t-fate mapping, NK1.1, and T1/ST2 expression.

Arg1⁺RNT⁻ cells in the fetal intestine are ILC precursors in the sense that they (1) lack the transcription factor profiles and surface proteins of mature ILC populations, and (2) have the capacity to differentiate into ILC lineages, but not T or B cells. However, intestinal Arg1⁺ ILC precursors in the fetus express T-bet and ROR γ t, and thus are unlike reported adult bone marrow Id2⁺ ILC precursors, which lack these transcription factors. This suggests that isolated Arg1⁺ ILC precursors are cells that are in the process of differentiation. These intestinal “intermediate ILC precursors” have restricted potency in culture compared to multipotent bone marrow precursors, since most wells from intestinal single cell cultures contain one type of differentiated ILC by day 6 (Constantinides et al, 2014; Klose et al, 2014). However, it is unclear whether intermediate ILC precursors enter the assay with fixed commitment to specific lineages. Further exploration into whether intermediate ILC precursors can be directed towards specific lineages by exogenous factors on a single cell basis would determine whether

these cells are terminally committed. Retinoic acid may be a candidate for intermediate ILC precursor skewing, since this metabolite enhances L_{Ti4} numbers *in vitro* (van de Pavert et al, 2014). IL-15 and Notch ligands may be other possible candidates for guiding development towards ILC1 or ILC2 development. Interestingly, the proportions of ILC lineages *in vivo* do not reflect frequencies of lineages that develop from isolated intestinal intermediate ILC precursors *in vitro*, suggesting that the intestinal environment may affect ILC differentiation. Further studies are required to determine whether there are specific exogenous factors in tissue that can bias ILC precursor development.

Arg1⁺ intermediate ILC precursors in the fetal intestine are heterogeneous, for they express varying levels of T-bet and RORγt. 64% of intermediate ILC precursors express T-bet in a bimodal fashion, while about 50% of Arg1⁺ precursors express low levels of RORγt. Whether differential levels of transcription factors are associated with differentiation into specific lineages is unknown, since this heterogeneity is only identified in fixed cells. Identifying additional cell surface markers within this population will assist in determining whether there are subsets within the Arg1⁺ precursor pool. In the case that transcription factor expression within this population represents a spectrum of developmental states rather than specific subsets, single cell transcript analysis may be helpful in determining when lineage determination occurs.

Whether intermediate ILC precursors are present in the adult remains unclear. In adult mice, ILCs have a fairly long half-life in tissue: four weeks for ILC2s in the lung and 22-26 days for ILC3s in intestinal lamina propria (Nussbaum et al, 2013; Sawa et al, 2010). This suggests that at rest, adult ILC precursors may be more quiescent than precursors in fetal animals. It will be informative to determine the tissue-specificity and

transcription factor expression of ILC precursors post-birth during homeostasis and in conditions where ILC populations are required, such as during intestinal tertiary lymphoid development and inflammation. Identifying whether ILC numbers in adult tissue are sustained by *in situ* proliferation, entry of newly developed cells from bone marrow, or through the development of tissue-resident precursors is yet to be determined.

Why do ILCs develop in peripheral tissues?

Both ILC precursors from the fetal liver and intermediate ILC precursors from the fetal intestine have the capacity to generate ILC1s, ILC2s, and ILC3s. The advantages of having precursors develop outside of the fetal liver have not been investigated, but may involve organ-specific lineage skewing and temporal control of ILC development. For Peyer's patch organogenesis, having intermediate ILC precursors in the intestine may provide a way to regulate the strength of activating signals during different steps of development. It was previously shown that LT_i cell numbers during fetal life correlate with both the number and size of Peyer's patches in adulthood (Meier et al, 2007; van de Pavert et al, 2014). This suggests a model in which dispersed LT_i cell numbers must be kept below a certain threshold prior to Peyer's patch development to prevent excessive numbers of activated sites, while a second threshold must be reached soon after in a localized manner, in order to maintain and enhance LT β R signaling at the anlage. Intermediate ILC precursors lack detectable levels of LT $\alpha_1\beta_2$ and thus should not be able to directly alter the numbers of Peyer's patches induced. However, these cells preferentially accumulate at the developing Peyer's patch and can differentiate into ILC3s that may be capable of amplifying stromal activation (Fig.1). Determining whether

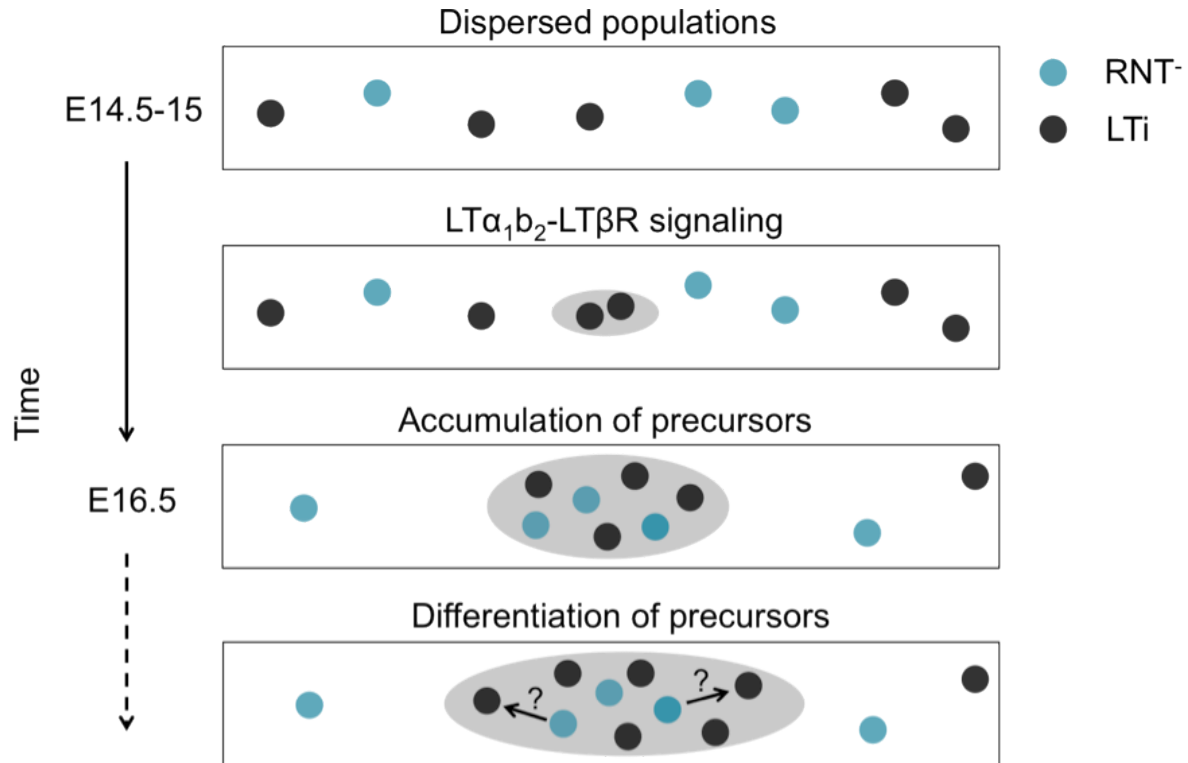


Figure 1. Model of precursor localization during Peyer's patch development. Both LTi cells (black circles) and ILC precursors (blue circles) are dispersed at E14.5-15 in proximal and middle regions of the intestine. Between E15.5 and E16.5, $LT\alpha_1\beta_2^+$ LTi cells activate stromal cells at the anlage to produce chemokines and adhesion molecules. By E16.5, ILC precursors are found to preferentially accumulate at the anlage compared to adjacent regions. While stromal production of CXCL13 and CCL21 induce chemotaxis of additional LTi cells towards the anlage, precursors lack CXCR5 and CCR7 and thus accumulate due to unknown factors. Precursors have the capacity to differentiate into mature ILC lineages, possibly including $LT\alpha_1\beta_2^+$ LTi cells that may further amplify activation at the developing Peyer's patch.

these cells contribute in this manner will require testing whether precursors at the anlage differentiate into LTi cells *in vivo*, as well as testing the effects of blocking precursor accumulation on Peyer's patch size and follicle number.

What determines the location of a developing intestinal lymphoid organ?

A major difference between lymph node and Peyer's patch organogenesis is the predictability of where these organs develop. While lymph nodes exist in specific anatomical sites, Peyer's patches do not develop in fixed locations along the proximal-distal axis of the small intestine (Alden et al, 2012). Additionally, the total number of Peyer's patches differs between mice within a single litter. However, Peyer's patch development is not completely stochastic, since it is still regulated in two ways: (1) these organs only develop along the anti-mesenteric axis (Cupedo, 2011), and (2) Peyer's patch development occurs in a sequential manner starting at the proximal end of the intestine and ending at the distal end (Adachi et al, 1997).

In Chapter 3, I show that LTi cells and intermediate ILC precursors are preferentially dispersed in proximal and middle regions of the small intestine at E14.5-15 and along the anti-mesenteric axis at E16.5, suggesting that the location of developing Peyer's patches may be partially regulated by where LTi cells are most abundant. Factors that retain these cells along the anti-mesenteric axis are not dependent on $LT\alpha 1\beta 2$ -based stromal activation, since LTi and $Arg1^+RNT^-$ cells localize along this region in the absence of *Lta*. Also, the LTi-attracting chemokines CXCL13, CCL19, and CCL21 are unlikely to be required, since ILC precursors do not express detectable receptors for these factors. Future studies may look towards fractionating intestines of *Lta*^{-/-} animals to determine stromal gene expression in regions that are

associated with greater numbers of ILC populations. Also, determining whether ILCs shift distally in *Lta*^{-/-} animals between E15.5-E18.5 would be informative as to whether this generalized LTi localization also correlates with distal developing Peyer's patches. It remains possible that ILCs are deposited on the anti-mesenteric axis as they enter tissue, although hematopoietic cells in the intestine move dynamically before Peyer's patch development, suggesting that additional factors may still be necessary to retain these populations (Veiga-Fernandes et al, 2007). Additionally, isolated lymphoid follicles (ILFs) develop post birth along the anti-mesenteric intestinal wall in naïve mice, indicating that there are stromal differences between the mesenteric and anti-mesenteric zones of the intestine that persist into adulthood (Hamada et al, 2002). Identifying factors that control LTi regionalization independent of *Lta* will give insight into how the positioning of gut lymphoid tissue organogenesis is regulated.

Use of RORyt-cre mice

The RORyt-cre transgenic mouse is used in studies that require lineage tracing or deletion of specific genes in both T cells and RORyt-expressing ILCs. However, these mice are prone to germline transmission of floxed out alleles. Male breeders containing both RORyt-cre and Rosa26-floxSTOP-RFP give rise to a percentage of progeny that express cre-independent RFP in all cells, indicating that there is variegated RORyt expression in male germ cells. To prevent germline transmission, a breeding scheme in which female breeders carry both RORyt-cre and the floxed allele, while male breeders only express the floxed allele, should be adopted. Studies using these mice to delete specific genes should describe breeding strategies, and provide evidence that cre-negative cells have intact floxed alleles.

During the analysis of Arg1⁺ precursors, RORγt reporter and RORγt protein expression were found to not completely overlap. Arg1⁺RNT⁻ cells, which lack RORγt fate mapping (fm), consist of RORγt protein-expressing cells. This incomplete reporting is not due to inefficiency of cre-induced floxing activity, since RORγt^{GFP} knock in-knock out reporter mice show similar patterns of expression. Instead, the lack of fluorescent protein expression in Arg1⁺RNT⁻ cells in these reporter mice may be due to low RORγt gene expression, or temporal delays as RORγt⁺RNT⁻ cells begin expressing this gene. This restricted reporting proved to be useful in distinguishing two distinct populations of RORγt protein-expressing cells in the fetal intestine. RORγt^{fm+} are LTi cells based on transcriptional and functional definitions. These T-bet⁻RORγt^{hi}GATA3^{low} cells express CXCR5 and CCR7, which are used in chemotaxis to the anlage, and LTα1β2, which is required for stromal activation at the developing Peyer's patch. In comparison, RORγt protein-expressing RORγt^{fm-} cells express more T-bet and GATA3 than LTi cells, and lack LTi-associated chemokine receptors and LTα1β2. These data reveal that incomplete RORγt detection by available reporter mice has utility in differentiating between LTi and intermediate ILC precursors in fetal tissue.

Arg1 expression in adult ILCs

Arginase-I is expressed by adult ILC1s, ILC2s, and ILC3s, but there are differences in the frequency of enzyme-expressing cells within each innate lymphoid group. In the case of ILC2s, >95% of these cells express Arg1 during homeostasis and helminth-induced inflammation in the adult. In contrast, adult ILC3s in cryptopatches include both Arg1⁺ and Arg1⁻ cells at rest. Although it is unclear why there is heterogeneity in Arg1 expression in adult ILCs, recent work has indicated that Arg1

gene expression in ILCs requires GATA3 (Yagi et al, 2014). These data are intriguing, since ILC2s express the highest levels of GATA3 when compared to other ILC populations, and also have the highest frequency of Arg1 expressers. How expression of this enzyme is regulated in these different innate lymphoid populations warrants further investigation.

The function of Arg1 in adult ILC2s is unclear. In the lung, Arg1 is highly expressed in tissue during *N. brasiliensis*-induced inflammation due to induction in alternatively activated macrophages and increased total numbers of ILC2s. Arg1 expression is not required by either of these populations for normal collagen production or worm clearance (Barron et al, 2013). Additionally, ILC2s express IL-5 and IL-13 normally in the absence of Arg1, and thus appear to function normally without this enzyme. It remains possible that IL-5 or eosinophils are required for Arg1-mediated effects on tissue, since the homozygous Red (IL-5)-cre mice used to delete Arg1 in ILC2s lack both of these components. However, since alternatively activated macrophages have over 10-fold more Arg1 activity than ILC2s per cell, it is unlikely that Arg1 expression by ILC2s is required for normal immune and tissue responses during strong type 2 responses. Whether there are functional consequences of deleting *Arg1* in ILC2s during homeostasis is unknown. In the naïve lung, ILC2s aggregate around collagen-rich areas near airways, and whether these niches are altered by Arg1-deficiency should be investigated (Nussbaum et al, 2013). ILC2s also produce IL-5 and IL-13 in naïve mice, indicating that there are additional roles for these cells during homeostasis that need to be dissected. Identifying these functions and determining whether they are altered in the absence of Arg1 are questions for future study.

In contrast to ILC2s, Arg1 is only expressed by a subset of ILC3s. Whether Arg1⁺ and Arg1⁻ ILC3s are functionally different subsets, represent different stages of ILC3 development or activation, or are derived from different types of ILC precursors is unclear. Investigating differences in cytokine production, transcription factors, LT $\alpha_1\beta_2$ expression, and timing of seeding will be informative as to whether these are two distinct populations. CD4 expression and *Ahr* dependence in different LT_i-like populations demonstrate that these cells consist of different subsets, but whether Arg1 is correlated with any of these specific groups is unknown. Determining whether these populations can be differentiated by Arg1 expression may provide insight into the different functions of these subsets of innate lymphoid cells.

References

Adachi S, Yoshida H, Kataoka H, Nishikawa S (1997) Three distinctive steps in Peyer's patch formation of murine embryo. *Int Immunol* **9**(4): 507-514

Alden K, Timmis J, Andrews PS, Veiga-Fernandes H, Coles MC (2012) Pairing experimentation and computational modeling to understand the role of tissue inducer cells in the development of lymphoid organs. *Front Immunol* **3**: 172

Atkinson DE (1992) Functional Roles of Urea Synthesis in Vertebrates. *Physiological Zoology* **65**(2): 243-267

Bando JK, Nussbaum JC, Liang HE, Locksley RM (2013) Type 2 innate lymphoid cells constitutively express arginase-I in the naive and inflamed lung. *J Leukoc Biol* **94**(5): 877-884

Barron L, Smith AM, El Kasmi KC, Qualls JE, Huang X, Cheever A, Borthwick LA, Wilson MS, Murray PJ, Wynn TA (2013) Role of arginase 1 from myeloid cells in th2-dominated lung inflammation. *PLoS One* **8**(4): e61961

Boos MD, Yokota Y, Eberl G, Kee BL (2007) Mature natural killer cell and lymphoid tissue-inducing cell development requires Id2-mediated suppression of E protein activity. *J Exp Med* **204**(5): 1119-1130

Camberis M, Le Gros G, Urban J, Jr. (2003) Animal model of *Nippostrongylus brasiliensis* and *Heligmosomoides polygyrus*. *Curr Protoc Immunol* **Chapter 19**: Unit 19 12

Cella M, Fuchs A, Vermi W, Facchetti F, Otero K, Lennerz JK, Doherty JM, Mills JC, Colonna M (2009) A human natural killer cell subset provides an innate source of IL-22 for mucosal immunity. *Nature* **457**(7230): 722-725

Cherrier M, Sawa S, Eberl G (2012) Notch, Id2, and RORgammat sequentially orchestrate the fetal development of lymphoid tissue inducer cells. *J Exp Med* **209**(4): 729-740

Colegio OR, Chu NQ, Szabo AL, Chu T, Rhebergen AM, Jairam V, Cyrus N, Brokowski CE, Eisenbarth SC, Phillips GM, Cline GW, Phillips AJ, Medzhitov R (2014) Functional polarization of tumour-associated macrophages by tumour-derived lactic acid. *Nature*

Constantinides MG, McDonald BD, Verhoef PA, Bendelac A (2014) A committed precursor to innate lymphoid cells. *Nature*

Cooper MD, Alder MN (2006) The evolution of adaptive immune systems. *Cell* **124**(4): 815-822

Corraliza IM, Campo ML, Soler G, Modolell M (1994) Determination of arginase activity in macrophages: a micromethod. *J Immunol Methods* **174**(1-2): 231-235

Cupedo TC, M.C.; Viega-Fernandes, H. (2011) Structure and development of Peyer's patches in humans and mice. *Developmental Biology of Peripheral Lymphoid Organs part 3*: 97-106

de Boer J, Williams A, Skavdis G, Harker N, Coles M, Tolaini M, Norton T, Williams K, Roderick K, Potocnik AJ, Kioussis D (2003) Transgenic mice with hematopoietic and lymphoid specific expression of Cre. *Eur J Immunol* **33**(2): 314-325

De Luca A, Zelante T, D'Angelo C, Zagarella S, Fallarino F, Spreca A, Iannitti RG, Bonifazi P, Renauld JC, Bistoni F, Puccetti P, Romani L (2010) IL-22 defines a novel immune pathway of antifungal resistance. *Mucosal Immunol* **3**(4): 361-373

De Togni P, Goellner J, Ruddle NH, Streeter PR, Fick A, Mariathasan S, Smith SC, Carlson R, Shornick LP, Strauss-Schoenberger J, et al. (1994) Abnormal development of peripheral lymphoid organs in mice deficient in lymphotoxin. *Science* **264**(5159): 703-707

Dzhagalov I, Giguere V, He YW (2004) Lymphocyte development and function in the absence of retinoic acid-related orphan receptor alpha. *J Immunol* **173**(5): 2952-2959

Eberl G (2005) Inducible lymphoid tissues in the adult gut: recapitulation of a fetal developmental pathway? *Nat Rev Immunol* **5**(5): 413-420

Eberl G, Littman DR (2004) Thymic origin of intestinal alphabeta T cells revealed by fate mapping of RORgammat+ cells. *Science* **305**(5681): 248-251

Eberl G, Marmon S, Sunshine MJ, Rennert PD, Choi Y, Littman DR (2004) An essential function for the nuclear receptor RORgamma(t) in the generation of fetal lymphoid tissue inducer cells. *Nat Immunol* **5**(1): 64-73

El Kasmi KC, Qualls JE, Pesce JT, Smith AM, Thompson RW, Henao-Tamayo M, Basaraba RJ, Konig T, Schleicher U, Koo MS, Kaplan G, Fitzgerald KA, Tuomanen EI, Orme IM, Kanneganti TD, Bogdan C, Wynn TA, Murray PJ (2008) Toll-like receptor-induced arginase 1 in macrophages thwarts effective immunity against intracellular pathogens. *Nat Immunol* **9**(12): 1399-1406

Erle DJ, Sheppard D (2014) The cell biology of asthma. *J Cell Biol* **205**(5): 621-631

Fonseca-Pereira D, Arroz-Madeira S, Rodrigues-Campos M, Barbosa IA, Domingues RG, Bento T, Almeida AR, Ribeiro H, Potocnik AJ, Enomoto H, Veiga-Fernandes H (2014) The neurotrophic factor receptor RET drives haematopoietic stem cell survival and function. *Nature*

Fuchs A, Vermi W, Lee JS, Lonardi S, Gilfillan S, Newberry RD, Cella M, Colonna M (2013) Intraepithelial type 1 innate lymphoid cells are a unique subset of IL-12- and IL-15-responsive IFN-gamma-producing cells. *Immunity* **38**(4): 769-781

Futterer A, Mink K, Luz A, Kosco-Vilbois MH, Pfeffer K (1998) The lymphotoxin beta receptor controls organogenesis and affinity maturation in peripheral lymphoid tissues. *Immunity* **9**(1): 59-70

Ginhoux F, Greter M, Leboeuf M, Nandi S, See P, Gokhan S, Mehler MF, Conway SJ, Ng LG, Stanley ER, Samokhvalov IM, Merad M Fate mapping analysis reveals that adult microglia derive from primitive macrophages. *Science* **330**(6005): 841-845

Gordon SM, Chaix J, Rupp LJ, Wu J, Madera S, Sun JC, Lindsten T, Reiner SL (2012) The transcription factors T-bet and Eomes control key checkpoints of natural killer cell maturation. *Immunity* **36**(1): 55-67

Halim TY, MacLaren A, Romanish MT, Gold MJ, McNagny KM, Takei F (2012) Retinoic-acid-receptor-related orphan nuclear receptor alpha is required for natural helper cell development and allergic inflammation. *Immunity* **37**(3): 463-474

Hamada H, Hiroi T, Nishiyama Y, Takahashi H, Masunaga Y, Hachimura S, Kaminogawa S, Takahashi-Iwanaga H, Iwanaga T, Kiyono H, Yamamoto H, Ishikawa H (2002) Identification of multiple isolated lymphoid follicles on the antimesenteric wall of the mouse small intestine. *J Immunol* **168**(1): 57-64

Herbert DR, Holscher C, Mohrs M, Arendse B, Schwegmann A, Radwanska M, Leeto M, Kirsch R, Hall P, Mossmann H, Claussen B, Forster I, Brombacher F (2004) Alternative macrophage activation is essential for survival during schistosomiasis and downmodulates T helper 1 responses and immunopathology. *Immunity* **20**(5): 623-635

Hesse M, Modolell M, La Flamme AC, Schito M, Fuentes JM, Cheever AW, Pearce EJ, Wynn TA (2001) Differential regulation of nitric oxide synthase-2 and arginase-1 by type 1/type 2 cytokines in vivo: granulomatous pathology is shaped by the pattern of L-arginine metabolism. *J Immunol* **167**(11): 6533-6544

Hoeffel G, Wang Y, Greter M, See P, Teo P, Malleret B, Leboeuf M, Low D, Oller G, Almeida F, Choy SH, Grisotto M, Renia L, Conway SJ, Stanley ER, Chan JK, Ng LG, Samokhvalov IM, Merad M, Ginhoux F (2012) Adult Langerhans cells derive predominantly from embryonic fetal liver monocytes with a minor contribution of yolk sac-derived macrophages. *J Exp Med* **209**(6): 1167-1181

Honda K, Nakano H, Yoshida H, Nishikawa S, Rennert P, Ikuta K, Tamechika M, Yamaguchi K, Fukumoto T, Chiba T, Nishikawa SI (2001) Molecular basis for hematopoietic/mesenchymal interaction during initiation of Peyer's patch organogenesis. *J Exp Med* **193**(5): 621-630

Hoshino K, Kashiwamura S, Kuribayashi K, Kodama T, Tsujimura T, Nakanishi K, Matsuyama T, Takeda K, Akira S (1999) The absence of interleukin 1 receptor-related T1/ST2 does not affect T helper cell type 2 development and its effector function. *J Exp Med* **190**(10): 1541-1548

Hoyler T, Klose CS, Souabni A, Turqueti-Neves A, Pfeifer D, Rawlins EL, Voehringer D, Busslinger M, Diefenbach A (2012) The transcription factor GATA-3 controls cell fate and maintenance of type 2 innate lymphoid cells. *Immunity* **37**(4): 634-648

Iyer RK, Yoo PK, Kern RM, Rozengurt N, Tsoa R, O'Brien WE, Yu H, Grody WW, Cederbaum SD (2002) Mouse model for human arginase deficiency. *Mol Cell Biol* **22**(13): 4491-4498

Kanamori Y, Ishimaru K, Nanno M, Maki K, Ikuta K, Nariuchi H, Ishikawa H (1996) Identification of novel lymphoid tissues in murine intestinal mucosa where clusters of c-kit⁺ IL-7R⁺ Thy1⁺ lympho-hemopoietic progenitors develop. *J Exp Med* **184**(4): 1449-1459

Kaplan MH, Schindler U, Smiley ST, Grusby MJ (1996) Stat6 is required for mediating responses to IL-4 and for development of Th2 cells. *Immunity* **4**(3): 313-319

Kennedy MK, Glaccum M, Brown SN, Butz EA, Viney JL, Embers M, Matsuki N, Charrier K, Sedger L, Willis CR, Brasel K, Morrissey PJ, Stocking K, Schuh JC, Joyce S, Peschon JJ (2000) Reversible defects in natural killer and memory CD8 T cell lineages in interleukin 15-deficient mice. *J Exp Med* **191**(5): 771-780

Klose CS, Flach M, Mohle L, Rogell L, Hoyler T, Ebert K, Fabiunke C, Pfeifer D, Sexl V, Fonseca-Pereira D, Domingues RG, Veiga-Fernandes H, Arnold SJ, Busslinger M, Dunay IR, Tanriver Y, Diefenbach A (2014) Differentiation of Type 1 ILCs from a Common Progenitor to All Helper-like Innate Lymphoid Cell Lineages. *Cell* **157**(2): 340-356

Klose CS, Kiss EA, Schwierzeck V, Ebert K, Hoyler T, d'Hargues Y, Goppert N, Croxford AL, Waisman A, Tanriver Y, Diefenbach A (2012) A T-bet gradient controls the fate and function of CCR6-ROR γ mat⁺ innate lymphoid cells. *Nature* **494**(7436): 261-265

Koni PA, Sacca R, Lawton P, Browning JL, Ruddle NH, Flavell RA (1997) Distinct roles in lymphoid organogenesis for lymphotoxins alpha and beta revealed in lymphotoxin beta-deficient mice. *Immunity* **6**(4): 491-500

Kreymborg K, Etzensperger R, Dumoutier L, Haak S, Rebollo A, Buch T, Heppner FL, Renaud JC, Becher B (2007) IL-22 is expressed by Th17 cells in an IL-23-dependent fashion, but not required for the development of autoimmune encephalomyelitis. *J Immunol* **179**(12): 8098-8104

Lee JS, Cella M, McDonald KG, Garlanda C, Kennedy GD, Nukaya M, Mantovani A, Kopan R, Bradfield CA, Newberry RD, Colonna M (2012) AHR drives the development of gut ILC22 cells and postnatal lymphoid tissues via pathways dependent on and independent of Notch. *Nat Immunol* **13**(2): 144-151

Luche H, Weber O, Nageswara Rao T, Blum C, Fehling HJ (2007) Faithful activation of an extra-bright red fluorescent protein in "knock-in" Cre-reporter mice ideally suited for lineage tracing studies. *Eur J Immunol* **37**(1): 43-53

Luther SA, Ansel KM, Cyster JG (2003) Overlapping roles of CXCL13, interleukin 7 receptor alpha, and CCR7 ligands in lymph node development. *J Exp Med* **197**(9): 1191-1198

Medzhitov R, Janeway C, Jr. (2000) Innate immunity. *N Engl J Med* **343**(5): 338-344

Meier D, Bornmann C, Chappaz S, Schmutz S, Otten LA, Ceredig R, Acha-Orbea H, Finke D (2007) Ectopic lymphoid-organ development occurs through interleukin 7-mediated enhanced survival of lymphoid-tissue-inducer cells. *Immunity* **26**(5): 643-654

Molofsky AB, Nussbaum JC, Liang HE, Van Dyken SJ, Cheng LE, Mohapatra A, Chawla A, Locksley RM (2013) Innate lymphoid type 2 cells sustain visceral adipose tissue eosinophils and alternatively activated macrophages. *J Exp Med* **210**(3): 535-549

Mombaerts P, Iacomini J, Johnson RS, Herrup K, Tonegawa S, Papaioannou VE (1992) RAG-1-deficient mice have no mature B and T lymphocytes. *Cell* **68**(5): 869-877

Moro K, Yamada T, Tanabe M, Takeuchi T, Ikawa T, Kawamoto H, Furusawa J, Ohtani M, Fujii H, Koyasu S (2010) Innate production of T(H)2 cytokines by adipose tissue-associated c-Kit(+)/Sca-1(+) lymphoid cells. *Nature* **463**(7280): 540-544

Morris SM, Jr. (2002) Regulation of enzymes of the urea cycle and arginine metabolism. *Annu Rev Nutr* **22**: 87-105

Munder M (2009) Arginase: an emerging key player in the mammalian immune system. *Br J Pharmacol* **158**(3): 638-651

Munder M, Eichmann K, Modolell M (1998) Alternative metabolic states in murine macrophages reflected by the nitric oxide synthase/arginase balance: competitive regulation by CD4+ T cells correlates with Th1/Th2 phenotype. *J Immunol* **160**(11): 5347-5354

Nair MG, Cochrane DW, Allen JE (2003) Macrophages in chronic type 2 inflammation have a novel phenotype characterized by the abundant expression of Ym1 and Fizz1 that can be partly replicated in vitro. *Immunol Lett* **85**(2): 173-180

Neill DR, Wong SH, Bellosi A, Flynn RJ, Daly M, Langford TK, Bucks C, Kane CM, Fallon PG, Pannell R, Jolin HE, McKenzie AN (2010) Nuocytes represent a new innate effector leukocyte that mediates type-2 immunity. *Nature* **464**(7293): 1367-1370

Nussbaum JC, Van Dyken SJ, von Moltke J, Cheng LE, Mohapatra A, Molofsky AB, Thornton EE, Krummel MF, Chawla A, Liang HE, Locksley RM (2013) Type 2 innate lymphoid cells control eosinophil homeostasis. *Nature* **502**(7470): 245-248

Okabe Y, Medzhitov R (2014) Tissue-specific signals control reversible program of localization and functional polarization of macrophages. *Cell* **157**(4): 832-844

Okuda M, Togawa A, Wada H, Nishikawa S (2007) Distinct activities of stromal cells involved in the organogenesis of lymph nodes and Peyer's patches. *J Immunol* **179**(2): 804-811

Ota N, Wong K, Valdez PA, Zheng Y, Crellin NK, Diehl L, Ouyang W (2011) IL-22 bridges the lymphotoxin pathway with the maintenance of colonic lymphoid structures during infection with *Citrobacter rodentium*. *Nat Immunol* **12**(10): 941-948

Pauleau AL, Rutschman R, Lang R, Pernis A, Watowich SS, Murray PJ (2004) Enhancer-mediated control of macrophage-specific arginase I expression. *J Immunol* **172**(12): 7565-7573

Pesce JT, Ramalingam TR, Mentink-Kane MM, Wilson MS, El Kasmi KC, Smith AM, Thompson RW, Cheever AW, Murray PJ, Wynn TA (2009) Arginase-1-expressing macrophages suppress Th2 cytokine-driven inflammation and fibrosis. *PLoS Pathog* **5**(4): e1000371

Price AE, Liang HE, Sullivan BM, Reinhardt RL, Eisley CJ, Erle DJ, Locksley RM (2010) Systemically dispersed innate IL-13-expressing cells in type 2 immunity. *Proc Natl Acad Sci U S A* **107**(25): 11489-11494

Rankin LC, Groom JR, Chopin M, Herold MJ, Walker JA, Mielke LA, McKenzie AN, Carotta S, Nutt SL, Belz GT (2013) The transcription factor T-bet is essential for the development of NKp46+ innate lymphocytes via the Notch pathway. *Nat Immunol* **14**(4): 389-395

Reece JJ, Siracusa MC, Scott AL (2006) Innate immune responses to lung-stage helminth infection induce alternatively activated alveolar macrophages. *Infect Immun* **74**(9): 4970-4981

Reese TA, Liang HE, Tager AM, Luster AD, Van Rooijen N, Voehringer D, Locksley RM (2007) Chitin induces accumulation in tissue of innate immune cells associated with allergy. *Nature* **447**(7140): 92-96

- Rothberg S (1958) Possible significance of elevated arginase activity in psoriasis scales. *Ann N Y Acad Sci* **73**(5): 1004-1012
- Rutschman R, Lang R, Hesse M, Ihle JN, Wynn TA, Murray PJ (2001) Cutting edge: Stat6-dependent substrate depletion regulates nitric oxide production. *J Immunol* **166**(4): 2173-2177
- Sandler NG, Mentink-Kane MM, Cheever AW, Wynn TA (2003) Global gene expression profiles during acute pathogen-induced pulmonary inflammation reveal divergent roles for Th1 and Th2 responses in tissue repair. *J Immunol* **171**(7): 3655-3667
- Satoh-Takayama N, Lesjean-Pottier S, Vieira P, Sawa S, Eberl G, Vosshenrich CA, Di Santo JP (2010) IL-7 and IL-15 independently program the differentiation of intestinal CD3-NKp46+ cell subsets from Id2-dependent precursors. *J Exp Med* **207**(2): 273-280
- Satoh-Takayama N, Vosshenrich CA, Lesjean-Pottier S, Sawa S, Lochner M, Rattis F, Mention JJ, Thiam K, Cerf-Bensussan N, Mandelboim O, Eberl G, Di Santo JP (2008) Microbial flora drives interleukin 22 production in intestinal NKp46+ cells that provide innate mucosal immune defense. *Immunity* **29**(6): 958-970
- Sawa S, Cherrier M, Lochner M, Satoh-Takayama N, Fehling HJ, Langa F, Di Santo JP, Eberl G (2010) Lineage relationship analysis of RORgammat+ innate lymphoid cells. *Science* **330**(6004): 665-669
- Schatz DG, Ji Y (2011) Recombination centres and the orchestration of V(D)J recombination. *Nat Rev Immunol* **11**(4): 251-263
- Shi O, Morris SM, Jr., Zoghbi H, Porter CW, O'Brien WE (2001) Generation of a mouse model for arginase II deficiency by targeted disruption of the arginase II gene. *Mol Cell Biol* **21**(3): 811-813
- Shinkai Y, Rathbun G, Lam KP, Oltz EM, Stewart V, Mendelsohn M, Charron J, Datta M, Young F, Stall AM, et al. (1992) RAG-2-deficient mice lack mature lymphocytes owing to inability to initiate V(D)J rearrangement. *Cell* **68**(5): 855-867
- Spits H, Artis D, Colonna M, Diefenbach A, Di Santo JP, Eberl G, Koyasu S, Locksley RM, McKenzie AN, Mebius RE, Powrie F, Vivier E (2013) Innate lymphoid cells--a proposal for uniform nomenclature. *Nat Rev Immunol* **13**(2): 145-149
- Spits H, Cupedo T (2012) Innate lymphoid cells: emerging insights in development, lineage relationships, and function. *Annu Rev Immunol* **30**: 647-675
- Spits H, Di Santo JP (2011) The expanding family of innate lymphoid cells: regulators and effectors of immunity and tissue remodeling. *Nat Immunol* **12**(1): 21-27

Srivastava S, Ratha BK (2010) Does fish represent an intermediate stage in the evolution of ureotelic cytosolic arginase I? *Biochemical and Biophysical Research Communications* **391**(1): 1-5

Stein M, Keshav S, Harris N, Gordon S (1992) Interleukin 4 potentially enhances murine macrophage mannose receptor activity: a marker of alternative immunologic macrophage activation. *J Exp Med* **176**(1): 287-292

Takatori H, Kanno Y, Watford WT, Tato CM, Weiss G, Ivanov, II, Littman DR, O'Shea JJ (2009) Lymphoid tissue inducer-like cells are an innate source of IL-17 and IL-22. *J Exp Med* **206**(1): 35-41

Tenu JP, Lepoivre M, Moali C, Brollo M, Mansuy D, Boucher JL (1999) Effects of the new arginase inhibitor N(omega)-hydroxy-nor-L-arginine on NO synthase activity in murine macrophages. *Nitric Oxide* **3**(6): 427-438

van de Pavert SA, Ferreira M, Domingues RG, Ribeiro H, Molenaar R, Moreira-Santos L, Almeida FF, Ibiza S, Barbosa I, Goverse G, Labao-Almeida C, Godinho-Silva C, Konijn T, Schooneman D, O'Toole T, Mizze MR, Habani Y, Haak E, Santori FR, Littman DR, Schulte-Merker S, Dzierzak E, Simas JP, Mebius RE, Veiga-Fernandes H (2014) Maternal retinoids control type 3 innate lymphoid cells and set the offspring immunity. *Nature* **508**(7494): 123-127

van de Pavert SA, Olivier BJ, Goverse G, Vondenhoff MF, Greuter M, Beke P, Kusser K, Hopken UE, Lipp M, Niederreither K, Blomhoff R, Sitnik K, Agace WW, Randall TD, de Jonge WJ, Mebius RE (2009) Chemokine CXCL13 is essential for lymph node initiation and is induced by retinoic acid and neuronal stimulation. *Nat Immunol* **10**(11): 1193-1199

Veiga-Fernandes H, Coles MC, Foster KE, Patel A, Williams A, Natarajan D, Barlow A, Pachnis V, Kioussis D (2007) Tyrosine kinase receptor RET is a key regulator of Peyer's patch organogenesis. *Nature* **446**(7135): 547-551

Voehringer D, Shinkai K, Locksley RM (2004) Type 2 immunity reflects orchestrated recruitment of cells committed to IL-4 production. *Immunity* **20**(3): 267-277

Vonarbourg C, Mortha A, Bui VL, Hernandez PP, Kiss EA, Hoyler T, Flach M, Bengsch B, Thimme R, Holscher C, Honig M, Pannicke U, Schwarz K, Ware CF, Finke D, Diefenbach A (2010) Regulated expression of nuclear receptor ROR γ confers distinct functional fates to NK cell receptor-expressing ROR γ innate lymphocytes. *Immunity* **33**(5): 736-751

Welch JS, Escoubet-Lozach L, Sykes DB, Liddiard K, Greaves DR, Glass CK (2002) TH2 cytokines and allergic challenge induce Ym1 expression in macrophages by a STAT6-dependent mechanism. *J Biol Chem* **277**(45): 42821-42829

Wong SH, Walker JA, Jolin HE, Drynan LF, Hams E, Camelo A, Barlow JL, Neill DR, Panova V, Koch U, Radtke F, Hardman CS, Hwang YY, Fallon PG, McKenzie AN (2012) Transcription factor RORalpha is critical for nuocyte development. *Nat Immunol* **13**(3): 229-236

Yagi R, Zhong C, Northrup DL, Yu F, Bouladoux N, Spencer S, Hu G, Barron L, Sharma S, Nakayama T, Belkaid Y, Zhao K, Zhu J (2014) The transcription factor GATA3 is critical for the development of all IL-7Ralpha-expressing innate lymphoid cells. *Immunity* **40**(3): 378-388

Yokota Y, Mansouri A, Mori S, Sugawara S, Adachi S, Nishikawa S, Gruss P (1999) Development of peripheral lymphoid organs and natural killer cells depends on the helix-loop-helix inhibitor Id2. *Nature* **397**(6721): 702-706

Yoshida H, Honda K, Shinkura R, Adachi S, Nishikawa S, Maki K, Ikuta K, Nishikawa SI (1999) IL-7 receptor alpha+ CD3(-) cells in the embryonic intestine induces the organizing center of Peyer's patches. *Int Immunol* **11**(5): 643-655

Zimmermann N, King NE, Laporte J, Yang M, Mishra A, Pope SM, Muntel EE, Witte DP, Pegg AA, Foster PS, Hamid Q, Rothenberg ME (2003) Dissection of experimental asthma with DNA microarray analysis identifies arginase in asthma pathogenesis. *J Clin Invest* **111**(12): 1863-1874

Publishing Agreement

It is the policy of the University to encourage the distribution of all theses, dissertations, and manuscripts. Copies of all UCSF theses, dissertations, and manuscripts will be routed to the library via the Graduate Division. The library will make all theses, dissertations, and manuscripts accessible to the public and will preserve these to the best of their abilities, in perpetuity.

I hereby grant permission to the Graduate Division of the University of California, San Francisco to release copies of my thesis, dissertation, or manuscript to the Campus Library to provide access and preservation, in whole or in part, in perpetuity.

Author Signature  Date 8/26/2014